DEVELOPMENT OF A NOVEL ASSAY OF PROTEIN TYROSINE PHOSPHATASE ACTIVITY IN SINGLE CELLS USING CAPILLARY ELECTROPHORESIS

Ryan Matthew Phillips

A dissertation submitted to the faculty of the University of North Carolina at Chapel Hill in partial fulfillment of the requirements for the degree of Doctor of Philosophy in the School of Medicine (Pharmacology).

Chapel Hill
2013

Approved by:
Nancy L. Allbritton, M.D., Ph.D.
Lee M. Graves, Ph.D.
Gary L. Johnson, Ph.D.
David S. Lawrence, Ph.D.
Jen Jen Yeh, M.D.

Abstract

RYAN MATTHEW PHILLIPS: Development of a Novel Assay of Protein Tyrosine Phosphatase Activity in Single Cells Using Capillary Electrophoresis
(Under the direction of Nancy Allbritton, M.D., Ph.D.)

The inhalation of diesel exhaust particles has been linked to human diseases including airway inflammation, arrhythmias, heart attack, stroke, hypertension, and cancer. *In vitro* studies have implicated the inhibition of protein tyrosine phosphatases (PTPs) by diesel exhaust components as a contributor to the inflammatory processes underlying these conditions. A more complete mechanistic understanding of this phenomenon could be achieved by observing the effects of diesel exhaust particle inhalation on the airways of exposed living human subjects. While airway specimens can be obtained safely from these subjects by bronchial brushing, sample analysis is complicated by low total cell numbers, poor viability, and contamination with inflammatory cells and mucus. We present a novel approach to the analysis of these challenging samples at the single-cell level that provides a direct measure of PTP activity without sacrificing information about intercellular heterogeneity commonly lost by analysis of bulk lysates.

A fluorescent phosphopeptide substrate of PTPs was synthesized and an analytical separation was developed to resolve and quantify phosphorylated and nonphosphorylated peptide, as well as potential degradation products, using capillary electrophoresis with laser-induced fluorescence detection. Peptide dephosphorylation was then used as a measure of PTP activity in a variety of model systems including recombinant PTPN1 and PTPN2, A431 cell lysates, and single A431 cells. The reporter was also used to characterize the inhibition

of PTP activity in these systems by three toxic components of diesel exhaust particles: pervanadate, 1,2-naphthoquinone, and Zn^{2+}.

The PTP reporter was then applied to common model systems of airway biology. PTP activity, as well as inhibition by the toxins listed above, was quantified in immortalized BEAS-2B bronchial epithelial cells as well as cultured primary human airway epithelial cells. PTP activity was then measured in single cells obtained directly from a living human subject via bronchial brushing. The ability to analyze these small, heterogeneous samples of primary cells at the single-cell level demonstrates the power of this approach as new tool for the field of airway biology as well as for the broader study of PTP signaling.

.

Table of Contents

List of Tables

Table

List of Figures

Figure

List of Abbreviations and Symbols

βPDGFR:	platelet-derived growth factor receptor beta
μ_{ep}	electrophoretic mobility
ug	microgram(s)
uL	microliter(s)
μM	micromolar
°C	degrees Celsius
6-FAM	6-carboxyfluorescein
ADCC	antibody dependent cellular cytotoxicity
ALI	air-liquid interface
amol	attomole(s)
AP-1	activator protein 1
Asp	aspartic acid
ATP	adenosine triphosphate
AZ	Arizona
BB	bronchial brushing
BCa	bias-corrected and accelerated
BEBM	bronchial epithelial basal medium
BEGM	bronchial epithelial growth medium
BOC	tert-butoxycarbonyl
BSA	bovine serum albumin
CA	California
CAPS	N-cyclohexyl-3-aminopropanesulfonic acid
CDC	complement dependent cytolysis

Cdc25A	cell division cycle 25 homolog A
cDNA	complementary deoxyribonucleic acid
CE	capillary electrophoresis
CE-LIF	capillary electrophoresis with laser-induced fluorescence detection
CHCA	α-cyano-4-hydroxycinnamic acid
cm	centimeter(s)
cm^2	square centimeter(s)
Co	cobalt
CO_2	carbon dioxide
COOH	carboxylic acid
COPD	chronic obstructive pulmonary disease
CT	computed tomography
CTAB	cetyl trimethylammonium bromide
CZE	capillary zone electrophoresis
D	aspartic acid
DCM	dichloromethane
DEP	diesel exhaust particles
DIC	diisopropylcarbodiimide
DMEM	Dulbecco's Modified Eagle's Medium
DMF	dimethylformamide
DNA	deoxyribonucleic acid
DSP	dual-specificity phosphatase
DTT	dithiothreitol
E	glutamic acid
EDTA	ethylenediaminetetraacetic acid

ECB	extracellular buffer
e.g.	exempli gratia (for example)
EGF	epidermal growth factor
EGFR	epidermal growth factor receptor
Em	emission wavelength
EOF	electroosmotic flow
EpCAM	epithelial cell adhesion molecule
ESR1	estrogen receptor 1
eq	equivalent(s)
ERK	extracellular-signal-regulated kinase
Ex	excitation wavelength
FBS	fetal bovine serum
Fc	fragment crystallizable region
FDA	Federal Drug Administration
FISH	fluorescence in situ hybridization
fL	femtoliter
Fmoc	fluorenylmethyloxycarbonyl
fmol min^{-1} mg^{-1}	femtomoles per minute per milligram
FNA	fine needle aspiration
g	gram(s) or acceleration due to gravity
Gab1	GRB2-associated binding protein 1
Glu	glutamic acid
GPCR	G-protein coupled receptor
GRB2	growth factor receptor-bound protein 2
GSK-3β	glycogen synthase kinase 3 beta

GST	glutathione S-transferase
h	hour(s)
H_2O_2	hydrogen peroxide
hAEC	human airway epithelial cell(s)
HCl	hydrochloric acid
HCTU	2-(6-Chloro-1H-benzotriazole-1-yl)-1,1,3,3-tetramethylaminium hexafluorophosphate
HEPES	2-[4-(2-hydroxyethyl)piperazin-1-yl]ethanesulfonic acid
HER2	human epidermal growth factor receptor 2
HOBt	1-hydroxybenzotriazole
HPLC	high performance liquid chromatography
IC_{50}	concentration eliciting 50% inhibition
IL-8	interleukin 8
IHC	immunohistochemistry
IR	insulin receptor
JAK2	Janus kinase 2
JNK	c-Jun N-terminal kinase
KBM	keratinocyte basal medium
k_{cat}	turnover number
KCl	potassium chloride
KGM	keratinocyte growth medium
K_M	Michaelis constant
kV	kilovolt(s)
L	leucine
L858R	leucine residue 858 mutated to arginine
Leu	leucine

LIF	laser-induced fluorescence
M	molar
MA	Massachusetts
MALDI	matrix-assisted laser desorption ionization
MEKC	micellar electrokinetic chromatography
MeOH	methanol
MET	hepatocyte growth factor receptor
min	minute(s)
mg	milligram(s)
Mg	magnesium
$MgCl_2$	magnesium chloride
min	minute(s)
mL	milliliter(s)
mM	millimolar
Mn	manganese
$MnCl_2$	manganese chloride
mol	mole(s)
MOPS	3-morpholinopropane-1-sulfonic acid
mRNA	messenger ribonucleic acid
MS	mass spectrometry
Mtt	methyltrityl
myrTS13	myristoylated peptide reporter
n	sample size
N_2	nitrogen
NaCl	sodium chloride

NaOH	sodium hydroxide
NC	North Carolina
Nd:YAG	neodymium-doped yttrium aluminum garnet
NF-κB	nuclear factor kappa-light-chain-enhancer of activated B cells
Nle	norleucine
nM	nanomolar
nm	nanometer(s)
nmol min^{-1} mg^{-1}	nanomoles per minute per milligram
NSCLC	non-small cell lung cancer
OBt	benzotriazolyl
OR	Oregon
OtBu	O-tert-butyl
P	phosphorus
p	statistical p-value
PCR	polymerase chain reaction
PDAC	pancreatic ductal adenocarcinoma
PDMS	polydimethylsiloxane
pg	picogram(s)
PLC-γ1	phospholipase C gamma 1
PM	particulate matter
pmol min-1 mg-1	picomoles per minute per milligram
PS	penicillin/streptomycin
PTP	protein tyrosine phosphatase
PTPN1	protein tyrosine phosphatase, non-receptor type 1
PTPN2	protein tyrosine phosphatase, non-receptor type 2

pTS13	phosphorylated peptide reporter
PV	pervanadate
Q_1	first quartile
Q_3	third quartile
qPCR	quantitative polymerase chain reaction
R^2	correlation coefficient
rcf	relative centrifugal force
RNA	ribonucleic acid
ROS	reactive oxygen species
rpm	rotations per minute
RTK	receptor tyrosine kinase
RT-PCR	reverse transcriptase polymerase chain reaction
s	second(s)
SDS	sodium dodecyl sulfate
SDS-PAGE	sodium dodecyl sulfate polyacrylamide gel electrophoresis
Shc	Src homology domain 2 containing transforming protein
SOS	Son of Sevenless
SPPS	solid phase peptide synthesis
ssTS13	myristylated, disulfide linked peptide reporter
STAT3	signal transducer and activator of transcription 3
STAT5	signal transducer and activator of transcription 5
T790M	threonine residue 790 mutated to methionine
TBA	tetrabutylammonium phosphate
tBu	tert-butyl
TC-PTP	T-cell protein tyrosine phosphatase

TGR	Tentagel Rink
TKI	tyrosine kinase inhibitor
TOF	time of flight
TS13	nonphosphorylated peptide reporter
Tyr	tyrosine
TX	Texas
US	United States
V	volt(s)
V_{max}	maximum velocity
v/v	volume/volume
VEGFR	vascular endothelial growth factor receptor
Y	tyrosine
Zn	zinc

I. Introduction

Protein tyrosine phosphatases. The protein tyrosine phosphatase (PTP) gene family consists of at least 100 members encoding enzymes capable of dephosphorylating proteins.[1] The classical PTPs are specific for phosphotyrosine-containing substrates, while the dual-specificity phosphatases (DSPs) can act on phosphorylated tyrosine, serine, and threonine residues. All catalytically active members of the PTP family share a characteristic phosphate-binding motif and act via a common mechanism.[2] Briefly, a phosphotyrosine residue is brought into close proximity of the PTP catalytic cysteine by surrounding residues including an essential arginine. Nucleophilic attack of the phosphotyrosine phosphate atom by the cysteine, P-O bond cleavage, and protonation of the tyrosine side-chain oxygen by a nearby PTP aspartate yields a phosphocysteine intermediate, which is subsequently converted to cysteine and free phosphate through hydrolysis of the unstable S-P bond by water. While the key catalytic machinery is conserved across PTPs, variations in non-catalytic regions of the phosphatase domain can lead to differing substrate specificity. Members of the PTP family participate in many facets of cell signaling and have been implicated in a variety of human diseases.

PTP substrate recognition and specificity. The classical PTPs can be divided into receptor (RPTP) and non-receptor (PTPN) types. Although great structural variability exists between PTPs, the RPTPs comprise at minimum a phosphatase domain, a transmembrane region, and an extracellular region while the simplest PTPNs contain only a phosphatase

domain and adjacent unstructured regions.[3] The higher-order structure of the PTP domain is highly conserved across PTPNs and RPTPs.[4] Key features of the PTP domain include an absolutely conversed catalytic cysteine residue within the HCX_5R "PTP signature motif", a phosphotyrosine recognition loop containing a KNRY motif important for substrate recognition, a WPD loop containing an aspartic acid critical to the phosphatase mechanism, and a Q loop that stabilizes a catalytic water molecule.[5] While the major features and overall fold of PTP domains is well conserved, the surface residues as well as several areas involved in substrate binding are highly variable to afford specificity of substrate recognition and interactions with scaffold and adapter proteins. For instance, while the WPD loop is present across PTPs, specific residues within and adjacent to the loop determine the details of its structure and dynamics, which in turn affect substrate binding and catalysis.[6] Variable residues critical to PTP substrate recognition also include two residues immediately N-terminal to the tyrosine of the KNRY motif and residues within and adjacent to the secondary substrate-binding pocket found in some PTPs, including PTPN1. Ultimately, the physiological substrate specificity of PTPs involves residues near the active site and more distant residues in the PTP domain that ensure proper substrate orientation, as well as the presence of additional protein-protein interaction domains and proper subcellular localization of PTPs.[7]

Regulation of PTP activity. While PTPs are critical to proper cell signaling, they must be tightly regulated to ensure signal integrity. This regulation occurs through the control of PTP expression, the presence of necessary adaptors and scaffold proteins, spatial sequestration of PTPs, transient oxidative inhibition, and protection of phosphotyrosine

residues through protein binding.[8] The latter three mechanisms of regulation have the greatest bearing on the work presented herein and therefore warrant further discussion.

PTP activity can be regulated by targeting to specific regions of the cell, both to prevent undesirable dephosphorylation and to ensure proximity of PTPs to appropriate targets.[9] The former is illustrated by PTP-1B and TC-PTP, which both possess hydrophobic C-terminal regions that target the enzymes to membranes including the endoplasmic reticulum. While membrane-bound, these enzymes possess little to no enzymatic activity, but physiological cleavage of the targeting sequences results in soluble PTPs with significantly increased activity. Targeting of active PTPs to specific cellular subcompartments has been observed, including cytoskeletal localization of PTPH1 by the Band 4.1 domain,[10] as well as nuclear localization of PTPε by a removable N-terminal sequence[11] and SHP-1 through a C-terminal sequence not found in the closely related SHP-2, which consequently does not localize to the nucleus.[12] Because the physiological context of PTPs often involves spatial targeting within the cell, it is important to ensure that a reporter of PTP activity will be accessible to its enzyme of interest within the cell, and also underlines an important difference between measuring PTP activity in cell lysates and in intact cells.

A second important mechanism of PTP regulation involves the transient inactivation of PTP catalytic activity through oxidation. Catalysis by PTPs involves transfer of a phosphoryl group from a substrate tyrosine to the catalytic cysteine, in thiolate anion form ($R\text{-}S^-$), of the PTP.[13] This thiolate anion is highly susceptible to oxidation by reactive oxygen species generated secondary to growth factor receptor signaling and in response to cellular stresses such as ionizing radiation. Oxidation of the thiolate anion to the sulfenic acid (R-SOH) is reversible, while further oxidation to the sulphinic ($R\text{-}SO_2H$) and sulphonic (R-

SO_3H) acids is irreversible. To prevent permanent PTP inactivation, the sulfenic acid can react with the peptide backbone to form a sulfenamide bond (R-SN-R) or with reduced glutathione or another cysteine residue to form S-glutathionylated cysteine or a disulfide bond, respectively. All of these products are less susceptible to further oxidation than sulfenic acid and permit regulation of signaling through reversible inactivation of PTPs. Proper regulation of PTPs through transient oxidation occurs in the complex redox environment of the intact cell, further supporting the value of studying PTP activity and inhibition in intact cells rather than lysates.

A third mechanism of PTP regulation involves physical separation of the enzymes from potential substrates through protein domains that bind phosphotyrosine, primarily the phosphotyrosine-binding (PTB) and src-homology 2 (SH2) domains.[14] Both of these domains are non-catalytic protein-protein interaction modules that recognize and bind phosphorylated tyrosine residues, albeit in different contexts. The SH2 domain is found on a wide range of proteins including kinases, phosphatases, adaptors, transcription factors. The SH2 domain recognizes substrates containing phosphotyrosine, and specificity is determined by interactions between substrate residues C-terminal to the phosphotyrosine and variable residues in the SH2 domain.[15] PTB domains occur almost exclusively on proteins lacking kinase or phosphatase domains. While substrate specificity is less well described for PTB domains, substrates recognized by PTB domains typically contain an NPX(Y/pY) consensus sequence.[16] Interestingly, many PTB domains bind preferentially to nonphosphorylated tyrosine, and in some instances will also bind phosphoinositides. Also, while SH2 domains typically recognize linear, unfolded peptide sequences, PTB domains more commonly recognize structured regions of proteins.[17] While the differing contexts in which these

domains interact with phosphotyrosine contribute to the intricacy and complexity of cell signaling, both domains bind phosphotyrosine residues, simultaneously permitting signal transduction based on tyrosine phosphorylation status and preserving signals by physically preventing binding and subsequent dephosphorylation by PTPs.[18]

PTPN1. First reported by Tonks *et al*,[19] PTPN1 (PTP-1B) is one of the most studied of the non-receptor PTPs, and plays critical roles in cell physiology and homeostasis. PTPN1 modulates signal transduction through dephosphorylation of RTKs (*e.g.* βPDGFR,[20] EGFR,[21] IR[22]), cytoplasmic kinases (*e.g.* JAK2,[23] GSK-3β,[24] Src[25]), transcription factors (*e.g.* STAT5,[26] ESR1[27]) and adapter proteins (*e.g.* β-catenin,[28] p62Dok[29]). The broad signaling network of PTPN1 underlies its implication in disease processes including obesity, type II diabetes mellitus, cancer, and airway inflammation.[30-31]

While interest in PTPN1 activity and inhibition has fueled drug development efforts, few compounds have been tested *in vivo*.[32] The PTPN1 inhibitor Trodusquemine (MSI-1436) was shown to increase fat loss in murine models of obesity,[33] leading to Phase I clinical trials in healthy and obese diabetic individuals.[34] Ertiprotafib progressed through Phase II clinical trials as a potential treatment for Type II Diabetes Mellitus, but was abandoned due to undesirable off-target effects.[35] Finally, studies in mice suggest that PTPN1 inhibition with 7-bromo-6-difluoromethylphosphonate 3-naphthalenenitrile may protect against progression and metastasis of some breast cancers,[36] however this has not yet been demonstrated in humans and concerns exist about the complex nature of PTPN1 signaling and the potentially far-reaching implications of its inhibition.

PTPN2. PTPN2 (T-Cell Protein Tyrosine Phosphatase, TC-PTP) was originally described in T-cells, but is ubiquitously expressed in humans.[37] Significant structural and functional similarities have been noted between PTPN2 and PTPN1.[38] However, absence of these enzymes in mice result in different phenotypes,[39-40] and structural differences have been identified as potential targets for specific inhibitors.[41]

Cancer has been a major focus of studies linking PTPN2 to human disease. Absent or decreased PTPN2 is associated with tumorigenesis in certain forms of human T-cell acute lymphoblastic leukemia,[42] and breast cancer,[43] and inhibition of apoptosis in murine keratinocytes exposed to ultraviolet radiation.[44] Conversely, deceased PTPN2 function results in decreased viability and proliferation in murine B-cell lymphomas,[45] suggesting that PTPN2 can both promote and inhibit carcinogenesis.

This duality of action extends beyond cancer. Decreases in PTPN2 activity have been implicated in autoimmune disease due to insufficient regulation of T-cell receptor signaling,[46] and specifically in ulcerative colitis and Crohn's disease through disregulation of autophagy[47] and inflammatory signaling[48] in colonic epithelia. However, partial inhibition of PTPN2 appears to prevent the development of insulin resistance in type 2 diabetes.[49] The complicated implications of PTPN2 activity modulation may underlie the lack of clinical inhibitor development for this enzyme.

Diesel exhaust particles and human health. Cardiovascular disease is the leading cause of death in the US for both men and women, resulting in 34% of deaths in 2006.[50] While it is clear that genetic and dietary influences play a role in the development of cardiovascular disease, a less obvious contributor appears to be the very air we breathe,

particularly in areas with high levels of automobile and industrial pollution. Processes like diesel fuel combustion generate fine and ultrafine particulate matter (PM) that deposits in the airways when inhaled. Epidemiological studies have linked PM inhalation to increases in blood pressure,[51] decreased cardiac autonomic control,[52] and significantly increased risk of heart attack and stroke.[53]

While the details underlying these health effects has not been fully elucidated, PM exposure has been linked to increased extracellular signal-regulated kinase (ERK) dependent IL-8 secretion in airways,[54] as well as increases in NF-κB and AP-1 activation and phosphorylation of p38 and JNK kinases,[55] all indicative of an inflammatory response mechanism. Recently, PM exposure has been shown to increase reactive oxygen species (ROS) in cells, resulting in activation EGFR[56] and p38.[57] A major contributor to the signaling disruptions associated with PM is intracellular PTP inhibition, which can be accomplished by several mechanisms as a result of the complex chemistry of PM.[58]

Inhibition mechanisms of PTPs. Physiological redox cycling of the phosphoryl-accepting cysteine is key to phosphatase functionality and regulation, but non-physiological oxidation of PTPs has been noted as a mechanism of toxicity due to inhaled particulate matter (PM). Transition metals in PM (*e.g.* iron, zinc, vanadium)[59] can lead to ROS generation and oxidation of PTP active site cysteine residues.[60-62] Oxidation of PTPs has also been identified as a potentially tumorigenic consequence of ionizing radiation through ROS generation and reversible S-nitrosylation.[63-64] Exposure of cells to a ^{60}Co radiation source generated reactive nitrogen species and caused reversible S-nitrosylation of active-site

cysteines. Ultraviolet light has also been shown to oxidize these residues and inhibit PTPs secondary to reactive oxygen species generation.

A non-oxidative mechanism of PTP inhibition related to PM involves the covalent modification by quinones adsorbed to airborne particulates or formed intracellularly through metabolism of naphthalene.[65-66] Specifically, exposure of PTPN1 to 1,2-naphthoquinone has been shown by mass spectrometry to result in covalent modification of cysteine and histidine residues.[67] Non-oxidative inhibition can also result from binding of Zn^{2+} to the PTP active site.[68] It should be noted that, while quinones and zinc can modify PTP through non-oxidative mechanisms, these species are also implicated in cellular redox disruption through glutathione depletion.[69-70]

Sources of heterogeneity in cell populations. Investigations at the single cell level have shown a surprising level of heterogeneity, even within clonal populations. In genomically unstable populations such as tumor cell lines, heterogeneity can result from the accumulation of isolated, stochastic genetic mutations and subsequent phenotypic alterations over time.[71] However, non-genetic heterogeneity is also an important consideration, and can be subdivided into temporal and population heterogeneity.[72]

Temporal heterogeneity is the variation of some characteristic (*e.g.* protein expression) of a single cell over time. The relatively low total number of biomolecules such as a specific mRNA or receptor, combined with the potential for high levels of amplification during translation or signal transduction can allow small, stochastic variations within a cell to yield significant phenotypic changes.[73-74]

Population heterogeneity refers to temporally stable differences between clones. Computer modeling in conjunction with experimental validation suggests this phenomenon emerges from a combination of localized environmental fluctuations and subsequent cell-cell communication leading to adaptation such that while individual cells may differ, the net result of their signaling behavior maintains environmental homeostasis.[75]

While the variation among clonal populations of cells is a strong argument for pursuing techniques that measure signaling in single cells, the added complexity of tissue samples, whether from model organisms, human research subjects, or patients, provides further motivation. Tissues are by definition a mixture of distinct cell types and bulk analysis of a mixed population averages multiple layers of heterogeneity into a single "typical" readout. Two tissues of interest during this work were human bronchial brushings and tumor biopsies.

Airway structure and bronchial brushings. Healthy human airways serve a number of vital functions, including air conduction, response to irritants and pathogens, and repair of damaged tissue.[76] This variety of functions is accomplished by the interactions of a complex mixture of epithelia, fibroblasts, smooth muscle, neuroendocrine cells, lymphoid tissue, and extracellular matrix.[77] While the complexity of this system is vitally important, it also complicates the analysis of airway biopsy samples, particularly when obtained by techniques such as bronchial brushing which, while less invasive than surgical biopsies, also provide small specimens with limited cell viability.[78] Furthermore, this complexity is increased when studying disease processes of the airways due to the additional presence of acute or chronic inflammatory cells, excess mucous, and/or fibrosis.[79]

Measurement of enzyme activity with peptides. Peptides allow investigation into the impact of protein primary (and sometimes secondary) structure on behavior. While the interaction of a substrate peptide with an enzyme does not recapitulate potential higher order structure, peptides have been used to study a wide range of enzyme-catalyzed protein modifications (*e.g.* methylation,[80] acetylation,[81] ubiquitination,[82] proteolysis[83]), though further discussion herein will focus on phosphorylation and dephosphorylation.

Perhaps the most straightforward application of peptides for measuring phosphorylation is the monitoring of transfer of radioactive phosphate from [γ-^{32}P] ATP to a substrate peptide by a kinase. This approach is widely used with enzyme-specific[84] or generic peptide substrates (e.g. poly(Glu,Tyr) 4:1 copolymer)[85] to measure kinase activity. While a powerful technique, relatively high limits of detection (10^{-14}-10^{-18} mol) limit its utility in studying single cells. Peptide substrate phosphorylation is also assessed via Western blot with anti-phosphotyrosine antibodies.[86] The integration of SDS-PAGE with this approach affords separation and detection of multiple substrates. Drawbacks to this technique include costly antibodies and relatively large sample size requirements. Another powerful approach for evaluation of kinases using peptides is mass spectrometry. Using this analytical technique, naturally occurring[87] and synthetic peptides[88] alike can be identified by molecular weight from complex samples including cell lysates[89] and single cells[90].

Several approaches exist for development of peptide-based kinase sensors that exhibit a change in fluorescence in response to phosphorylation status. A two-step assay has been demonstrated in which a rhodamine-conjugated kinase substrate is incubated with a kinase, then with an aminopeptidase. Peptide cleavage by the aminopeptidase releases free

rhodamine 110 and results in a fluorescence increase, but serine-phosphorylation of the substrate prevents degradation and keeps the fluorophore in a conjugated, non-fluorescent state.[91] A single-step alternative for kinase sensing involves development of environmentally sensitive sensors in which phosphorylation in the presence of an appropriate soluble phospho-motif binding domain results in a changes in solvation or quenching interactions and induce a fluorescence increase.[92] Fluorogenic peptides have been used to measure phosphatase activity using tyrosine analogs that exhibit a fluorescence increase upon dephosphorylation[93] as well as designs in which serine-dephosphorylation leads to peptide cyclization and fluorophore release.[94]

Capillary electrophoresis. Jorgenson and Lukacs first demonstrated that free-zone electrophoresis could be performed in thin glass capillaries to provide high resolution separations.[95] Chief among the benefits described in this early work were the elimination of potentially adsorptive stabilizing media (gels, paper, etc.) and the elimination of thermal gradient formation as a major contributor to band broadening. Since this initial report, capillary electrophoresis (CE) has evolved into a powerful analytical technique with a wide range of applications.

The simplest form of capillary electrophoresis, in which analytes migrate in free solution, is known as capillary zone electrophoresis (CZE).[96] Analyte retention time in CZE is determined by the electrophoretic mobility (μ_{ep}) of each analyte, as well as the velocity and direction of electroosmotic flow (EOF), a bulk fluid flow that occurs when a potential is applied to an electrolyte-filled capillary. The μ_{ep} for a species is proportional to the ratio of its charge and Stokes radius, while the EOF in an unmodified capillary will be directed

toward the negative electrode with a velocity dependent on electric field strength as well as buffer pH, ionic strength, and viscosity.

While CZE is a powerful separation technique, the inclusion of micelle-forming additives in the background electrolyte, known as micellar electrokinetic capillary chromatography (MEKC), can aid in difficult separations by providing a pseudostationary phase. Under MEKC conditions, analytes migrate based on EOF and μ_{ep}, but may also interact with micelles through electrostatic as well as hydrophibic interations. The dynamic partitioning of analytes between free solution and large, relatively slow-moving micelles provides an additional parameter for distinguishing otherwise similar analytes.

Analytes in CE can be detected by a variety of methods including absorbance, conductivity, mass spectrometry, and fluorescence. Laser induced fluorescence (LIF) detection, in which fluorescent analytes are excited with a laser, can afford very high sensitivity on the order of 10^{-21} mol.[97] LIF detection is limited to detection of fluorescent analytes, which may necessitate careful selection or modification of analytes, but also eliminates the potentially confounding detection of contaminants such as assay constituents and cell debris.

The high separation efficiencies, sensitivity, and selective detection have made CE-LIF a powerful technique for single cell analysis.[98] This technique has been used to quantify intracellular levels of endogenous neurotransmitters in single neurons[99] and drug uptake in single leukemia cells.[100] CE-LIF has also been used to study metabolism of sugars,[101] gangliosides,[102] lipids,[103] and peptides[104] in single cells.

Analysis of fluorescent peptides using CE-LIF. While fluorogenic peptides can provide real-time information about phosphorylation, but as only one species is fluorescent, phosphorylated and nonphosphorylated reporter cannot be quantified simultaneously. This issue can be addressed using CE-LIF, which has been demonstrated for purified peptides, in vitro assays, cellular lysates, and single cells. Because fluorescence does not rely on phosphorylation status, both species can be quantified simultaneously. Peptides containing tryptophan or phenylalanine can be detected (ex: ~270 nm, em: 305 nm) without derivitization,[105] however this method lends itself to confounding from other biological components containing these residues. Derivitization of analytes with fluorophores permits detection at wavelengths unlikely to overlap significantly with native fluorescence. A wide range of reactive fluorophores are available for functionalization of the amines, hydroxyls, carboxylic acids, and sulfhydryls present on peptides and proteins (bioconjugate techniques), and many have been used in conjuction with CE-LIF either prior to electrophoresis (off-column) or within the capillary (on-column).[105] For analysis of synthetic peptides, fluorophores can be readily conjugated to the N-terminus or to reactive side chains such as lysine using standard SPPS.

Solid Phase Peptide Synthesis. Solid-phase peptide synthesis (SPPS) using N-α-fluorenylmethyloxycarbonyl (Fmoc) chemistry is a convenient, efficient, and widely utilized alternative to conventional organic synthesis. The overall workflow of Fmoc-based SPPS involves immobilization of the C-terminal amino acid to a resin bead followed by sequential deprotection of the N-terminus and peptide elongation through coupling of a soluble

carboxylic acid. The completed peptide is then cleaved from the resin for purification and characterization.[106]

Polystyrene resin beads serving as solid support for synthesis afford rapid reagent exchange and dramatically simplify multi-step syntheses. Beads can be functionalized with a variety of linkers to yield products with C-terminal moieties including amides, carboxylic acids, and sulfhydryl groups. Linker identity also dictates the conditions under which the peptide is removed from the resin. The acid-labile trialkoxybenzhydrylamine (Rink amide) linker was used for synthesis of the peptide amides TS13 and pTS13, while peptide acid fragments were synthesized using the highly acid-labile 2-chlorotrityl chloride linker.

Peptides often contain amines, carboxylic acids, hydroxyls, or sulfhydryl moieties that require chemical modification, in the form of orthogonal protecting groups, to avoid undesirable reactivity during synthesis. The use of N-α-fmoc protected amino acids prevents off-resin amide bond formation during peptide elongation. Groups such as tert-butyl (tBu), O-tert-butyl (OtBu), and tert-butoxycarbonyl (BOC) are commonly used to protect carboxylic acids, hydroxyls, and amines. These groups are removed during cleavage from the resin and thus are inappropriate for on-resin side-chain modification. However, protecting groups such as methyltrityl (Mtt) can be removed under otherwise minimally disruptive conditions and thus facilitate on-resin side-chain modifications.

While many strategies for peptide bond formation exist, one of the most common approaches involves benzotriazolyl (OBt) ester formation. Pre-incubation of an N-α-Fmoc protected amino acid with 1-hydroxybenzotriazole (HOBt) and an activator such as 2-(6-chloro-1H-benzotriazole-1-yl)-1,1,3,3-tetramethylaminium hexafluorophosphate (HCTU) or diisopropylcarbodiimide (DIC) results in the formation of an OBt ester at the α-carbonyl.

This ester is susceptible to nucleophilic attack by the N-terminal free amino of the resin-bound peptide, leading to peptide bond formation.

Origins of the TS13 and pTS13 sequences. The observation that tyrosine kinases preferentially phosphorylate sites with nearby acidic residues[107] led to investigation of numerous proteins as potential EGFR substrates, including human erythrocyte Band 3 Protein.[108] The acidic N-terminus of this protein served as the basis for the highest affinity EGFR peptide substrate known (K_m = 34 μM).[109-110] This peptide in turn was modified with an N-terminal fluorescein to produce TS13 and its phosphotyrosine-containing analogue pTS13.

A431 cells. The A431 cell line was cultivated from a human epidermoid carcinoma specimen by Giard and colleagues.[111] These cells produce large quantities of wild-type EGFR,[112] approximately 2.6 x 10^6 receptors/cell,[113] due to genetic amplification through chromosomal translocations.[114] These cells have been essential in the study of PTP activity and inhibition. Lee *et al* observed that treatment of A431 cells with EGF results in reversible PTP1B inhibition linked to a transient increase in intracellular H_2O_2.[115] The mechanism of this inhibition, PTP sulfenylation, was subsequently described in A431 lysates[116] and later in living A431 cells.[117] These cells have also been used to study the importance of PTPs in cell adhesion[118] and as transducers between GPCRs and RTKs.[119]

BEAS-2B cells. The BEAS-2B cell line was established and reported by Reddel and colleagues in 1988.[120] Normal human bronchial epithelial cells were obtained by autopsy

and exposed to Ad12-SV40 virus, resulting in immortalized, nontumorigenic bronchial epithelia that were continuously propagated in culture for over one year. While BEAS-2B cells are non-ciliated,[121] they bear similarities to primary epithelia cultured as a monolayer in terms of antioxidative capacity,[122] inflammatory response,[123] and matrix attachment.[124] These similarities have facilitated many studies of inflammatory signaling due to chronic disease as well as environmental exposures.[125-129]

Primary human airway epithelial cells (hAECs). In addition to immortalized cell lines, primary hAECs obtained from necropsy or living human subjects can be cultured used for airway biology research. While monolayers of these cultured cells are widely used to study airway physiology and disease, this approach does not fully recapitulate the conditions of human airways, in which cells exist at an air-liquid interface (ALI). While ALI cell culture techniques can be used to reproduce the native environment of primary airway cells, the rapid changes in transepithelial electrical resistance, differentiation potential, and heterogeneity that occur when these cells are grown in traditional culture[130] underline the value of approaches that allow analysis of signaling behavior as quickly as possible after tissue procurement without the need for cell culture.

References

1. Tonks, N. K., *Nat Rev Mol Cell Biol,* **2006,** *7,* 833-846.

2. Barford, D.; Das, A. K.; Egloff, M. P., *Annu Rev Biophys Biomol Struct,* **1998,** *27,* 133-164.

3. Tiganis, T.; Bennett, A. M., *Biochem J,* **2007,** *402,* 1-15.

4. Barr, A. J.; Ugochukwu, E.; Lee, W. H.; King, O. N.; Filippakopoulos, P.; Alfano, I.; Savitsky, P.; Burgess-Brown, N. A.; Muller, S.; Knapp, S., *Cell,* **2009,** *136,* 352-363.

5. Buist, A.; Zhang, Y. L.; Keng, Y. F.; Wu, L.; Zhang, Z. Y.; den Hertog, J., *Biochemistry,* **1999,** *38,* 914-922.

6. Brandao, T. A.; Johnson, S. J.; Hengge, A. C., *Arch Biochem Biophys,* **2012,** *525,* 53-59.

7. den Hertog, J., *Mech Dev,* **1999,** *85,* 3-14.

8. Tonks, N. K., *FEBS J,* **2013,** *280,* 346-378.

9. Mauro, L. J.; Dixon, J. E., *Trends Biochem Sci,* **1994,** *19,* 151-155.

10. Zhang, S. H.; Eckberg, W. R.; Yang, Q.; Samatar, A. A.; Tonks, N. K., *J Biol Chem,* **1995,** *270,* 20067-20072.

11. Kraut, J.; Volohonsky, G.; Toledano-Katchalski, H.; Elson, A., *Exp Cell Res,* **2002,** *281,* 182-189.

12. Poole, A. W.; Jones, M. L., *Cell Signal,* **2005,** *17,* 1323-1332.

13. den Hertog, J.; Groen, A.; van der Wijk, T., *Arch Biochem Biophys,* **2005,** *434,* 11-15.

14. Kaneko, T.; Joshi, R.; Feller, S. M.; Li, S. S., *Cell Commun Signal,* **2012,** *10,* 32.

15. Kaneko, T.; Huang, H.; Zhao, B.; Li, L.; Liu, H.; Voss, C. K.; Wu, C.; Schiller, M. R.; Li, S. S., *Sci Signal,* **2010,** *3,* ra34.

16. Yaffe, M. B., *Nat Rev Mol Cell Biol,* **2002,** *3,* 177-186.

17. Shoelson, S. E., *Curr Opin Chem Biol,* **1997,** *1,* 227-234.

18. Rotin, D.; Margolis, B.; Mohammadi, M.; Daly, R. J.; Daum, G.; Li, N.; Fischer, E. H.; Burgess, W. H.; Ullrich, A.; Schlessinger, J., *EMBO J,* **1992,** *11,* 559-567.

19. Tonks, N. K.; Diltz, C. D.; Fischer, E. H., *J Biol Chem,* **1988,** *263,* 6731-6737.

20. Klinghoffer, R. A.; Kazlauskas, A., *J Biol Chem,* **1995,** *270,* 22208-22217.

21. Flint, A. J.; Tiganis, T.; Barford, D.; Tonks, N. K., *Proc Natl Acad Sci U S A,* **1997,** *94,* 1680-1685.

22. Bandyopadhyay, D.; Kusari, A.; Kenner, K. A.; Liu, F.; Chernoff, J.; Gustafson, T. A.; Kusari, J., *J Biol Chem,* **1997,** *272,* 1639-1645.

23. Myers, M. P.; Andersen, J. N.; Cheng, A.; Tremblay, M. L.; Horvath, C. M.; Parisien, J. P.; Salmeen, A.; Barford, D.; Tonks, N. K., *J Biol Chem,* **2001,** *276,* 47771-47774.

24. Wang, Q. M.; Fiol, C. J.; DePaoli-Roach, A. A.; Roach, P. J., *J Biol Chem,* **1994,** *269,* 14566-14574.

25. Bjorge, J. D.; Pang, A.; Fujita, D. J., *J Biol Chem,* **2000,** *275,* 41439-41446.

26. Aoki, N.; Matsuda, T., *J Biol Chem,* **2000,** *275,* 39718-39726.

27. Arnold, S. F.; Obourn, J. D.; Jaffe, H.; Notides, A. C., *Mol Endocrinol,* **1995,** *9,* 24-33.

28. Balsamo, J.; Arregui, C.; Leung, T.; Lilien, J., *J Cell Biol,* **1998,** *143,* 523-532.

29. Dube, N.; Cheng, A.; Tremblay, M. L., *Proc Natl Acad Sci U S A,* **2004,** *101,* 1834-1839.

30. Dube, N.; Tremblay, M. L., *Biochim Biophys Acta,* **2005,** *1754,* 108-117.

31. Berdnikovs, S.; Pavlov, V. I.; Abdala-Valencia, H.; McCary, C. A.; Klumpp, D. J.; Tremblay, M. L.; Cook-Mills, J. M., *J Immunol,* **2012,** *188,* 874-884.

32. Scott, L. M.; Lawrence, H. R.; Sebti, S. M.; Lawrence, N. J.; Wu, J., *Curr Pharm Des,* **2010,** *16,* 1843-1862.

33. Lantz, K. A.; Hart, S. G.; Planey, S. L.; Roitman, M. F.; Ruiz-White, I. A.; Wolfe, H. R.; McLane, M. P., *Obesity (Silver Spring),* **2010,** *18,* 1516-1523.

34. Clinicaltrials.gov. http://clinicaltrials.gov/ct2/results?term=MSI-1436&Search=Search (accessed February 21, 2013).

35. Erbe, D. V.; Wang, S.; Zhang, Y. L.; Harding, K.; Kung, L.; Tam, M.; Stolz, L.; Xing, Y.; Furey, S.; Qadri, A.; Klaman, L. D.; Tobin, J. F., *Mol Pharmacol,* **2005,** *67,* 69-77.

36. Julien, S. G.; Dube, N.; Read, M.; Penney, J.; Paquet, M.; Han, Y.; Kennedy, B. P.; Muller, W. J.; Tremblay, M. L., *Nat Genet,* **2007,** *39,* 338-346.

37. Doody, K. M.; Bourdeau, A.; Tremblay, M. L., *Immunol Rev,* **2009,** *228,* 325-341.

38. Romsicki, Y.; Kennedy, B. P.; Asante-Appiah, E., *Arch Biochem Biophys,* **2003,** *414,* 40-50.

39. Klaman, L. D.; Boss, O.; Peroni, O. D.; Kim, J. K.; Martino, J. L.; Zabolotny, J. M.; Moghal, N.; Lubkin, M.; Kim, Y. B.; Sharpe, A. H.; Stricker-Krongrad, A.; Shulman, G. I.; Neel, B. G.; Kahn, B. B., *Mol Cell Biol,* **2000,** *20,* 5479-5489.

40. You-Ten, K. E.; Muise, E. S.; Itie, A.; Michaliszyn, E.; Wagner, J.; Jothy, S.; Lapp, W. S.; Tremblay, M. L., *J Exp Med,* **1997,** *186,* 683-693.

41. Iversen, L. F.; Moller, K. B.; Pedersen, A. K.; Peters, G. H.; Petersen, A. S.; Andersen, H. S.; Branner, S.; Mortensen, S. B.; Moller, N. P., *J Biol Chem,* **2002,** *277,* 19982-19990.

42. Kleppe, M.; Lahortiga, I.; El Chaar, T.; De Keersmaecker, K.; Mentens, N.; Graux, C.; Van Roosbroeck, K.; Ferrando, A. A.; Langerak, A. W.; Meijerink, J. P.; Sigaux, F.; Haferlach, T.; Wlodarska, I.; Vandenberghe, P.; Soulier, J.; Cools, J., *Nat Genet,* **2010,** *42*, 530-535.

43. Shields, B. J.; Wiede, F.; Gurzov, E. N.; Wee, K.; Hauser, C.; Zhu, H. J.; Molloy, T. J.; O'Toole, S. A.; Daly, R. J.; Sutherland, R. L.; Mitchell, C. A.; McLean, C. A.; Tiganis, T., *Mol Cell Biol,* **2013,** *33*, 557-570.

44. Kim, D. J.; Tremblay, M. L.; Digiovanni, J., *PLoS One,* **2010,** *5*, e10290.

45. Young, R. M.; Polsky, A.; Refaeli, Y., *Blood,* **2009,** *114*, 5016-5023.

46. Zikherman, J.; Weiss, A., *J Clin Invest,* **2011,** *121*, 4618-4621.

47. Scharl, M.; Wojtal, K. A.; Becker, H. M.; Fischbeck, A.; Frei, P.; Arikkat, J.; Pesch, T.; Kellermeier, S.; Boone, D. L.; Weber, A.; Loessner, M. J.; Vavricka, S. R.; Fried, M.; McCole, D. F.; Rogler, G., *Inflamm Bowel Dis,* **2012,** *18*, 1287-1302.

48. Scharl, M.; McCole, D. F.; Weber, A.; Vavricka, S. R.; Frei, P.; Kellermeier, S.; Pesch, T.; Fried, M.; Rogler, G., *Gut,* **2011,** *60*, 189-197.

49. Fukushima, A.; Loh, K.; Galic, S.; Fam, B.; Shields, B.; Wiede, F.; Tremblay, M. L.; Watt, M. J.; Andrikopoulos, S.; Tiganis, T., *Diabetes,* **2010,** *59*, 1906-1914.

50. Lloyd-Jones, D.; Adams, R. J.; Brown, T. M.; Carnethon, M.; Dai, S.; De Simone, G.; Ferguson, T. B.; Ford, E.; Furie, K.; Gillespie, C.; Go, A.; Greenlund, K.; Haase, N.; Hailpern, S.; Ho, P. M.; Howard, V.; Kissela, B.; Kittner, S.; Lackland, D.; Lisabeth, L.; Marelli, A.; McDermott, M. M.; Meigs, J.; Mozaffarian, D.; Mussolino, M.; Nichol, G.; Roger, V.; Rosamond, W.; Sacco, R.; Sorlie, P.; Stafford, R.; Thom, T.; Wasserthiel-Smoller, S.; Wong, N. D.; Wylie-Rosett, J., *Circulation,* **2009**.

51. Bartoli, C. R.; Wellenius, G. A.; Diaz, E. A.; Lawrence, J.; Coull, B. A.; Akiyama, I.; Lee, L. M.; Okabe, K.; Verrier, R. L.; Godleski, J. J., *Environ Health Perspect,* **2008,** *117*.

52. Liao, D.; Duan, Y.; Whitsel, E. A.; Zheng, Z. J.; Heiss, G.; Chinchilli, V. M.; Lin, H. M., *Am J Epidemiol,* **2004,** *159*, 768-777.

53. Miller, K. A.; Siscovick, D. S.; Sheppard, L.; Shepherd, K.; Sullivan, J. H.; Anderson, G. L.; Kaufman, J. D., *N Engl J Med,* **2007,** *356,* 447-458.

54. Samet, J. M.; Rappold, A.; Graff, D.; Cascio, W. E.; Berntsen, J. H.; Huang, Y. C.; Herbst, M.; Bassett, M.; Montilla, T.; Hazucha, M. J.; Bromberg, P. A.; Devlin, R. B., *Am J Respir Crit Care Med,* **2009,** *179,* 1034-1042.

55. Pourazar, J.; Mudway, I. S.; Samet, J. M.; Helleday, R.; Blomberg, A.; Wilson, S. J.; Frew, A. J.; Kelly, F. J.; Sandstrom, T., *Am J Physiol Lung Cell Mol Physiol,* **2005,** *289,* L724-730.

56. Samet, J. M.; Dewar, B. J.; Wu, W.; Graves, L. M., *Toxicol Appl Pharmacol,* **2003,** *191,* 86-93.

57. Wang, T.; Chiang, E. T.; Moreno-Vinasco, L.; Lang, G. D.; Pendyala, S.; Samet, J. M.; Geyh, A. S.; Breysse, P. N.; Chillrud, S. N.; Natarajan, V.; Garcia, J. G., *Am J Respir Cell Mol Biol,* **2009**.

58. Samet, J. M.; Tal, T. L., *Annu Rev Pharmacol Toxicol,* **2010,** *50,* 215-235.

59. Costa, D. L.; Dreher, K. L., *Environ Health Perspect,* **1997,** *105 Suppl 5,* 1053-1060.

60. Walther, U. I.; Wilhelm, B.; Walther, S.; Muckter, H.; Fichtl, B., *Biol Trace Elem Res,* **2000,** *78,* 163-177.

61. Park, S.; Nam, H.; Chung, N.; Park, J. D.; Lim, Y., *Toxicol In Vitro,* **2006,** *20,* 851-857.

62. Huyer, G.; Liu, S.; Kelly, J.; Moffat, J.; Payette, P.; Kennedy, B.; Tsaprailis, G.; Gresser, M. J.; Ramachandran, C., *J Biol Chem,* **1997,** *272,* 843-851.

63. Barrett, D. M.; Black, S. M.; Todor, H.; Schmidt-Ullrich, R. K.; Dawson, K. S.; Mikkelsen, R. B., *J Biol Chem,* **2005,** *280,* 14453-14461.

64. Xu, Y.; Shao, Y.; Voorhees, J. J.; Fisher, G. J., *J Biol Chem,* **2006,** *281,* 27389-27397.

65. Xia, T.; Korge, P.; Weiss, J. N.; Li, N.; Venkatesen, M. I.; Sioutas, C.; Nel, A., *Environ Health Perspect,* **2004,** *112,* 1347-1358.

66. O'Brien, P. J., *Chem Biol Interact*, **1991,** *80*, 1-41.

67. Iwamoto, N.; Sumi, D.; Ishii, T.; Uchida, K.; Cho, A. K.; Froines, J. R.; Kumagai, Y., *J Biol Chem*, **2007,** *282*, 33396-33404.

68. Haase, H.; Maret, W., *Exp Cell Res*, **2003,** *291*, 289-298.

69. Kumagai, Y.; Shinkai, Y.; Miura, T.; Cho, A. K., *Annu Rev Pharmacol Toxicol*, **2012,** *52*, 221-247.

70. Walther, U. I.; Walther, S. C.; Muckter, H.; Fichtl, B., *Biol Trace Elem Res*, **2008,** *122*, 216-228.

71. Masramon, L.; Vendrell, E.; Tarafa, G.; Capella, G.; Miro, R.; Ribas, M.; Peinado, M. A., *J Cell Sci*, **2006,** *119*, 1477-1482.

72. Huang, S., *Development*, **2009,** *136*, 3853-3862.

73. Kaern, M.; Elston, T. C.; Blake, W. J.; Collins, J. J., *Nat Rev Genet*, **2005,** *6*, 451-464.

74. Elowitz, M. B.; Levine, A. J.; Siggia, E. D.; Swain, P. S., *Science*, **2002,** *297*, 1183-1186.

75. Stockholm, D.; Benchaouir, R.; Picot, J.; Rameau, P.; Neildez, T. M.; Landini, G.; Laplace-Builhe, C.; Paldi, A., *PLoS One*, **2007,** *2*, e394.

76. Knight, D., *Immunol Cell Biol*, **2001,** *79*, 160-164.

77. Cagle, P. T.; Allen, T. C.; Kerr, K. M., *Transbronchial and endobronchial biopsies*. Lippincott Williams & Wilkins: Philadelphia, 2009; p p.

78. Romagnoli, M.; Vachier, I.; Vignola, A. M.; Godard, P.; Bousquet, J.; Chanez, P., *Respir Med*, **1999,** *93*, 461-466.

79. Leslie, K. O.; Wick, M. R., *Practical Pulmonary Pathology: A Diagnostic Approach*. Saunders: Philadelphia, PA, 2011.

80. Murray, E. D., Jr.; Clarke, S., *J Biol Chem,* **1984,** *259,* 10722-10732.

81. Graham, L. D.; Packman, L. C.; Perham, R. N., *Biochemistry,* **1989,** *28,* 1574-1581.

82. Madden, M. M.; Song, W.; Martell, P. G.; Ren, Y.; Feng, J.; Lin, Q., *Biochemistry,* **2008,** *47,* 3636-3644.

83. Kim, Y. G.; Lone, A. M.; Nolte, W. M.; Saghatelian, A., *Proc Natl Acad Sci U S A,* **2012,** *109,* 8523-8527.

84. Fan, Y. X.; Wong, L.; Johnson, G. R., *Biochem J,* **2005,** *392,* 417-423.

85. Beebe, J. A.; Wiepz, G. J.; Guadarrama, A. G.; Bertics, P. J.; Burke, T. J., *J Biol Chem,* **2003,** *278,* 26810-26816.

86. Abe, M.; Kuroda, Y.; Hirose, M.; Watanabe, Y.; Nakano, M.; Handa, T., *Br J Pharmacol,* **2006,** *147,* 402-411.

87. Menschaert, G.; Vandekerckhove, T. T.; Baggerman, G.; Schoofs, L.; Luyten, W.; Van Criekinge, W., *J Proteome Res,* **2010,** *9,* 2051-2061.

88. Till, J. H.; Annan, R. S.; Carr, S. A.; Miller, W. T., *J Biol Chem,* **1994,** *269,* 7423-7428.

89. Bowley, E.; Mulvihill, E.; Howard, J. C.; Pak, B. J.; Gan, B. S.; O'Gorman, D. B., *BMC Biochem,* **2005,** *6,* 29.

90. Neupert, S.; Rubakhin, S. S.; Sweedler, J. V., *Chem Biol,* **2012,** *19,* 1010-1019.

91. Kupcho, K.; Somberg, R.; Bulleit, B.; Goueli, S. A., *Anal Biochem,* **2003,** *317,* 210-217.

92. Sharma, V.; Wang, Q.; Lawrence, D. S., *Biochim Biophys Acta,* **2008,** *1784,* 94-99.

93. Stanford, S. M.; Panchal, R. G.; Walker, L. M.; Wu, D. J.; Falk, M. D.; Mitra, S.; Damle, S. S.; Ruble, D.; Kaltcheva, T.; Zhang, S.; Zhang, Z. Y.; Bavari, S.; Barrios, A. M.; Bottini, N., *Proc Natl Acad Sci U S A,* **2012,** *109,* 13972-13977.

94. Xue, F.; Seto, C. T., *Org Lett*, **2010,** *12*, 1936-1939.

95. Jorgenson, J. W.; Lukacs, K. D., *Clin Chem*, **1981,** *27*, 1551-1553.

96. Weinberger, R., *Practical capillary electrophoresis*. 2nd ed.; Academic Press: San diego, CA, 2000; p xvii, 462 p.

97. Whitmore, C. D.; Olsson, U.; Larsson, E. A.; Hindsgaul, O.; Palcic, M. M.; Dovichi, N. J., *Electrophoresis*, **2007,** *28*, 3100-3104.

98. Lin, Y.; Trouillon, R.; Safina, G.; Ewing, A. G., *Anal Chem*, **2011,** *83*, 4369-4392.

99. Fuller, R. R.; Moroz, L. L.; Gillette, R.; Sweedler, J. V., *Neuron*, **1998,** *20*, 173-181.

100. Chen, Y.; Walsh, R. J.; Arriaga, E. A., *Anal Chem*, **2005,** *77*, 2281-2287.

101. Krylov, S. N.; Arriaga, E.; Zhang, Z.; Chan, N. W.; Palcic, M. M.; Dovichi, N. J., *J Chromatogr B Biomed Sci Appl*, **2000,** *741*, 31-35.

102. Essaka, D. C.; Prendergast, J.; Keithley, R. B.; Hindsgaul, O.; Palcic, M. M.; Schnaar, R. L.; Dovichi, N. J., *Neurochem Res*, **2012,** *37*, 1308-1314.

103. Jiang, D.; Sims, C. E.; Allbritton, N. L., *Faraday Discuss*, **2011,** *149*, 187-200; discussion 227-145.

104. Kovarik, M. L.; Allbritton, N. L., *Trends Biotechnol*, **2011,** *29*, 222-230.

105. Garcia-Campana, A. M.; Taverna, M.; Fabre, H., *Electrophoresis*, **2007,** *28*, 208-232.

106. Chan, W. C.; White, P. D., *Fmoc solid phase peptide synthesis : a practical approach*. Oxford University Press: New York, 2000; p xxiv, 346 p.

107. Hunter, T., *J Biol Chem*, **1982,** *257*, 4843-4848.

108. Shiba, T.; Akiyama, T.; Kadowaki, T.; Fukami, Y.; Tsuji, T.; Osawa, T.; Kasuga, M.; Takaku, F., *Biochem Biophys Res Commun*, **1986,** *135*, 720-727.

109. Guyer, C. A.; Woltjer, R. L.; Coker, K. J.; Staros, J. V., *Arch Biochem Biophys,* **1994,** *312,* 573-578.

110. Kaul, R. K.; Murthy, S. N.; Reddy, A. G.; Steck, T. L.; Kohler, H., *J Biol Chem,* **1983,** *258,* 7981-7990.

111. Giard, D. J.; Aaronson, S. A.; Todaro, G. J.; Arnstein, P.; Kersey, J. H.; Dosik, H.; Parks, W. P., *J Natl Cancer Inst,* **1973,** *51,* 1417-1423.

112. Ullrich, A.; Coussens, L.; Hayflick, J. S.; Dull, T. J.; Gray, A.; Tam, A. W.; Lee, J.; Yarden, Y.; Libermann, T. A.; Schlessinger, J.; et al., *Nature,* **1984,** *309,* 418-425.

113. Haigler, H.; Ash, J. F.; Singer, S. J.; Cohen, S., *Proc Natl Acad Sci U S A,* **1978,** *75,* 3317-3321.

114. Gill, G. N.; Weber, W.; Thompson, D. M.; Lin, C.; Evans, R. M.; Rosenfeld, M. G.; Gamou, S.; Shimizu, N., *Somat Cell Mol Genet,* **1985,** *11,* 309-318.

115. Lee, S. R.; Kwon, K. S.; Kim, S. R.; Rhee, S. G., *J Biol Chem,* **1998,** *273,* 15366-15372.

116. Lou, Y. W.; Chen, Y. Y.; Hsu, S. F.; Chen, R. K.; Lee, C. L.; Khoo, K. H.; Tonks, N. K.; Meng, T. C., *FEBS J,* **2008,** *275,* 69-88.

117. Paulsen, C. E.; Truong, T. H.; Garcia, F. J.; Homann, A.; Gupta, V.; Leonard, S. E.; Carroll, K. S., *Nat Chem Biol,* **2012,** *8,* 57-64.

118. Harder, K. W.; Moller, N. P.; Peacock, J. W.; Jirik, F. R., *J Biol Chem,* **1998,** *273,* 31890-31900.

119. Graness, A.; Hanke, S.; Boehmer, F. D.; Presek, P.; Liebmann, C., *Biochem J,* **2000,** *347,* 441-447.

120. Reddel, R. R.; Ke, Y.; Gerwin, B. I.; McMenamin, M. G.; Lechner, J. F.; Su, R. T.; Brash, D. E.; Park, J. B.; Rhim, J. S.; Harris, C. C., *Cancer Res,* **1988,** *48,* 1904-1909.

121. Gomperts, B. N.; Kim, L. J.; Flaherty, S. A.; Hackett, B. P., *Am J Respir Cell Mol Biol,* **2007,** *37,* 339-346.

122. Kinnula, V. L.; Yankaskas, J. R.; Chang, L.; Virtanen, I.; Linnala, A.; Kang, B. H.; Crapo, J. D., *Am J Respir Cell Mol Biol,* **1994,** *11,* 568-576.

123. McGovern, T.; Risse, P. A.; Tsuchiya, K.; Hassan, M.; Frigola, G.; Martin, J. G., *Am J Physiol Lung Cell Mol Physiol,* **2010,** *299,* L808-815.

124. Heijink, I. H.; Brandenburg, S. M.; Noordhoek, J. A.; Postma, D. S.; Slebos, D. J.; van Oosterhout, A. J., *Eur Respir J,* **2010,** *35,* 894-903.

125. Veranth, J. M.; Kaser, E. G.; Veranth, M. M.; Koch, M.; Yost, G. S., *Part Fibre Toxicol,* **2007,** *4,* 2.

126. Pichavant, M.; Charbonnier, A. S.; Taront, S.; Brichet, A.; Wallaert, B.; Pestel, J.; Tonnel, A. B.; Gosset, P., *J Allergy Clin Immunol,* **2005,** *115,* 771-778.

127. Chuang, C. Y.; Chang, C. H.; Huang, Y. L., *Inhal Toxicol,* **2009,** *21,* 153-167.

128. Ryter, S. W.; Lee, S. J.; Choi, A. M., *Expert Rev Respir Med,* **2010,** *4,* 573-584.

129. Fujisawa, T.; Kato, Y.; Atsuta, J.; Terada, A.; Iguchi, K.; Kamiya, H.; Yamada, H.; Nakajima, T.; Miyamasu, M.; Hirai, K., *J Allergy Clin Immunol,* **2000,** *105,* 126-133.

130. Stewart, C. E.; Torr, E. E.; Mohd Jamili, N. H.; Bosquillon, C.; Sayers, I., *J Allergy (Cairo),* **2012,** *2012,* 943982.

II. Measurement of Protein Tyrosine Phosphatase Activity in Single Cells by Capillary Electrophoresis

Overview

A fluorescent peptide substrate was used to measure dephosphorylation by protein tyrosine phosphatases (PTP) in cell lysates, and single cells and to investigate the effect of environmental toxins on PTP activity in these systems. Dephosphorylation of the substrate by PTPN1 and PTPN2 obeyed Michaelis-Menten kinetics, with K_M values of 770 ± 250 nM and 290 ± 54 nM, respectively. Dose-response curves and IC_{50} values were determined for the inhibition of these two enzymes by the environmental toxins Zn^{2+} and 1,2-naphthoquinone, as well as pervanadate. In A431 cell lysates, the reporter was a poor substrate for peptidases (degradation rate of 100 ± 8.2 fmol min^{-1} mg^{-1}) but an excellent substrate for phosphatases (dephosphorylation rate of 1.4 ± 0.3 nmol min^{-1} mg^{-1}). Zn^{2+}, 1,2-naphthoquinone and pervanadate inhibited dephosphorylation of the reporter in cell lysates with IC_{50} values of 470 nM, 35 μM, and 100 nM, respectively. Dephosphorylation of the reporter following loading into living single cells occurred at rates of at least 2 pmol min^{-1} mg^{-1}. When single cells were exposed to 1,2-naphthoquinone (50 μM), Zn^{2+} (100 μM), and pervanadate (1 mM), dephosphorylation was inhibited with median values and first and third quartile values of 41 (Q_1 = 0%, Q_3 = 96%), 50 (Q_1 = 46%, Q_3 = 74%), and 53% (Q_1 = 36%, Q_3 = 77%) , respectively, demonstrating both the impact of these toxic exposures on cell signaling and the heterogeneity of response between cells. This approach will provide a

valuable tool for the study of PTP dynamics, particularly in small, heterogeneous populations such as human biopsy specimens.

Introduction

The human genome encodes 107 protein tyrosine phosphatases (PTPs),[1] enzymes containing a catalytic cysteine residue capable of removing phosphoryl moieties from tyrosine residues on proteins. This enzyme family plays a critical role in maintaining proper cell signaling through its opposition of protein tyrosine kinases and dysregulation of these key enzymes is associated with many diseases, including type I diabetes mellitus, cancer, and rheumatoid arthritis.[2] PTP inhibition is also linked to the toxicity associated with inhalation of diesel exhaust particles (DEP), an important component of air pollution.[3] Combustion of diesel fuel by vehicles and industrial equipment produces fine particulate matter (diameter < 2.5 μm) containing a mixture that includes elemental carbon, polyaromatic hydrocarbons, and metals.[4] The deposition of these particles in small airways and alveoli is associated with numerous human health hazards including heart attacks, arrhythmias, chronic obstructive pulmonary disease (COPD), and asthma.[5] *In vitro* studies have linked DEP components to reactive oxygen species production[6] as well as direct inhibition of PTPs.[7]

Although studies on purified PTPs, cell lysates, and fixed tissue samples have provided valuable insight into the role of diesel exhaust particles in human disease, analysis of *ex vivo* samples acquired from human subjects remains challenging. Bronchial brushing (BB) is a well-established method of obtaining airway cells for analysis by dislodging them with a brush in conjunction with fiberoptic bronchoscopy.[8] Although BB samples are a valuable source of primary airway cells for research, the sample size is typically very limited

(0.8-3.6 x 10^4 cells).[9] The small sample size is further complicated by the specimen heterogeneity which in addition to the intact airway epithelia contains mucus, stromal tissue, and the remnants of cells killed during dislodging. To date, direct analysis of these specimens has focused on genetic techniques including fluorescence in situ hybridization (FISH),[10] RNA microarrays,[11] and polymerase chain reaction (PCR).[12] Although these approaches provide valuable information, new analytical tools for these BB specimens are required to provide additional information about the biochemistry of human airway cells.

The direct measurement of cell processes by chemical cytometry has the potential to provide unique advantages in the study of BB specimens. Although a wide range of chemical cytometry approaches exist,[13] the measurement of PTP activity in airway specimens must be compatible with very small numbers of heterogeneous primary cells, and single-cell CE-LIF is a promising approach to address this challenge. Sample heterogeneity is readily addressed by the selection and analysis of individual cells, while the high separation efficiency and detection limits approaching 10^{-21} mol[14] have made it possible to study many aspects of single cells, including protein and lipid kinase activity, proteolysis, nitric oxide release, and response to oxidative stress.[14-15] Because PTPs are part of a complicated signaling network, the ability to multiplex measurement of several enzymes is very attractive, and CE has been used for monochromatic detection of up to 20 analytes simultaneously[16] and multicolor systems have also been described.[17]

Herein we demonstrate the utility of single-cell capillary electrophoresis for the measurement of PTP activity in single intact cells, a technology well-suited for analysis of small heterogeneous samples such as that from a BB. We developed and validated a fluorescent peptide reporter of PTP activity and measured the kinetics of dephosphorylation

by two common model phosphatases. Additionally, we observed inhibition of these phosphatases by three toxins known to be present in diesel exhaust and then generated dose-response curves for the environmental toxins. A separation method for the peptide and all possible fluorescent cleavage products was developed so that peptide cleavage in cell lysates and intact cells could be quantified. The lifetime of the peptide, dephosphorylation rate and influence of environmental toxins was assessed in A431 cell lysates. Finally, the peptide lifetime and the dephosphorylation rate in single A431 cells were quantified in the presence and absence of environmental toxins. This work was published in Analytical Chemistry.[18]

Experimental Section

Materials. N-α-(9-fluorenylmethyloxycarbonyl) protected amino acids, 2-(6-Chloro-1H-benzotriazole-1-yl)-1,1,3,3-tetramethylaminium hexafluorophosphate (HCTU), N-hydroxybenzotriazole (HOBt), 1,3-diisopropylcarbodiimide (DIC), and TentaGel Rink (TGR) resin were obtained from EMD Novabiochem. 6-Carboxyfluorescein (6-FAM) was obtained from Anaspec and recombinant phosphatases were purchased from Millipore. Bovine serum albumin (BSA) was from Calbiochem, Dulbecco's Modified Eagle's Medium (DMEM) from Cellgro, penicillin/streptomycin (PS) and 0.25% Trypsin from Gibco, and fetal bovine serum (FBS) from Atlanta Biologicals. Sylgard 184 polydimethylsiloxane (PDMS) was purchased from Dow Corning. All other chemicals were purchased from either Sigma or Fisher.

Peptide Synthesis and Characterization. The full-length substrate peptide, termed "pTS13" when phosphorylated and "TS13" when nonphosphorylated, was synthesized using standard solid-phase peptide synthesis techniques on TGR resin, while peptide acid

fragments were synthesized on 2-chlorotritylchloride resin, both using an automated peptide synthesizer (PS3, Protein Technologies, Tuscon, AZ). Peptide synthesis was accomplished by coupling 5 equivalents (eq) of N-α-Fmoc protected amino acid in N,N-dimethylformamide (DMF) with HCTU (5 eq) and N-methylmorpholine (10 eq) for 20 min. Unreacted amines were then acetylated using 1:1 acetic anhydride in DMF. N-terminal deprotection was achieved using two 15 min incubations with 30% (v/v) piperidine in DMF. Coupling of 6-carboxyfluorescein (3 eq) to the peptide N-terminus was performed manually using DIC (3 eq) and HOBt (3 eq) in DMF for 24 h, followed by two 15 min incubations with 30% (v/v) piperidine in DMF. Cleavage from TGR resin and side-chain deprotection was accomplished by incubating in 95% TFA, 2.5% triisopropylsilane, 2.5% water for 3 h at room temperature. TFA was evaporated under a stream of N_2 gas, followed by peptide precipitation with ice-cold diethyl ether. Peptides were allowed to dry overnight then dissolved in water for purification by C18 reversed-phase HPLC, followed by lyophilization and storage at -20 ^{0}C. Peptide molecular weight was confirmed by matrix-assisted laser desorption ionization time-of-flight mass spectrometry (MALDI-TOF-MS) using an AB4800 (Applied Biosystems, Carlsbad, CA) and α-cyano-4-hydroxycinnamic acid (CHCA) matrix.

Capillary Electrophoresis. Separation of the peptide reporter based on phosphorylation status was performed using 140 mM borate, 150 mM SDS, 50 mM NaCl in a bare fused-silica capillary [30 μm inner diameter, 350 μm outer diameter, (Polymicro Technologies, Phoenix, AZ)] . Separations were performed on either a ProteomeLab PA800 (Beckman Coulter, Fullerton, CA) with a 30 cm long capillary, or on a customized system with a 38 cm long capillary. Capillaries were conditioned before use with successive rinses of 0.1 M NaOH (12 h), water (1 h), 0.1 M HCl (6 h), and water (12 h). Laser-induced

fluorescence (excitation: 488 nm, detection: 532 nm) was used for detection of fluorescent peptides. On the commercial system, samples were loaded into the capillary by applying positive pressure (0.5 psi for 5 s) to the capillary inlet followed by separation at 8 kV (267 V/cm) with a negative outlet. On the customized system, electrokinetic sample loading (79 V/cm for 5 s, negative outlet) was followed by separation at 10 kV (263 V/cm). Data were acquired with software written in Labview (National Instruments, Austin, TX) or with 32 Karat software (Beckman Coulter, Brea, CA) and analyzed using Matlab (The Mathworks, Natick, MA) and Origin (OriginLab, Northampton, MA) software.

Recombinant Phosphatase Activity Assay. Dephosphorylation of peptide by recombinant human PTPN1 and PTPN2 was observed with and without the PTP inhibitors pervanadate, 1,2-naphthoquinone, and zinc. The PTPN1 used was a human, N-terminal GST-tagged construct (residues 1-321) while the PTPN2 was a human construct (residues 1-341), both expressed in *E. coli*. For some reactions, PTP was incubated with the environmental toxins pervanadate, 1,2-naphthoquinone, or zinc pyrithione for 10 min at 21 °C prior to addition of pTS13. PTP was diluted (11.1 pg/ μL for PTPN1, 2.8 pg/ μL for PTPN2) in 90 μL of reaction buffer (60 mM 4-(2-hydroxyethyl)-1-piperazineethanesulfonic acid (HEPES), 150 mM sodium chloride, 0.17 mM dithiothreitol, 0.83 (v/v)% glycerol, 0.017 (w/v) % BSA, 0.002% Brij-35, pH 7.2), followed by addition of pTS13 in water to final peptide concentrations of 780 nM or 280 nM for reactions with PTPN1 or PTPN2, respectively, and the reactions were allowed to proceed at 21 °C for 10 min. Reactions were terminated by addition of an equal volume of 200 μM HCl and samples were stored at -20 °C prior to analysis. CE of each sample was performed and the percent dephosphorylated

peptide was calculated as the area of the dephosphorylated peptide peak divided by the total area of all peptide peaks on the electropherogram.

Determination of Kinetic Constants. The Michaelis constant, K_M, and maximum reaction velocity, V_{max}, were determined for the interaction of recombinant PTPN1 and PTPN2 with pTS13 by measuring initial reaction rates over a range of pTS13 concentrations. Recombinant PTPN1 (3.3-6.7 pg/ μL) or PTPN2 (0.67-1.7 pg/ μL) in reaction buffer was incubated with pTS13 (110-1390 nM) as described above. The amount of product formed was measured by CE at multiple time points for each substrate concentration and initial rates were plotted versus substrate concentration. Nonlinear regression of the data using the Michaelis-Menten equation was performed using Origin software and kinetic constants were calculated.

Cell Culture. A431 cells, a human epidermoid carcinoma cell line expressing high levels of EGFR,[19] were grown in a humidified atmosphere at 37 °C and 5% CO_2 . Cells were cultured in 75 cm^2 tissue culture flasks in DMEM (10 (v/v) % FBS, 1 (v/v) % P/S) and were passaged at 60-80% confluency using 0.25% trypsin.

Cell lysate experiments. A431 cells from two 75 cm^2 culture flasks were trypsinized for 5 min, diluted in DMEM, centrifuged 2 min at 800 x g, and then washed twice with PBS and pelleted. After removal of the supernatant, the pellet was resuspended in lysis buffer (20 mM HEPES, 1% Triton X-100, 10% Glycerol, 200mM NaCl, 5 mM β-glycerophosphate) with 1 (v/v) % Sigma Protease Inhibitor Cocktail. Lysate was mixed end-over-end for 20 min, followed by centrifugation at 15000x g for 40 min. The supernatant was transferred to a fresh 1.5 mL tube and protein concentration was measured as previously reported[20]. Lysates were then diluted to 10 mg/mL total protein and stored at -20 ^{0}C for up to 1 month.

For phosphatase assays, cell lysates were diluted to 111 ng/μL total protein in 90 μL of reaction buffer (described above) with or without environmental toxins. After 10 min of pre-incubation, pTS13 in water was added to a final concentration of 280 nM and the reaction was allowed to proceed for 90 s. Reactions were stopped by addition of an equal volume of 200 μM HCl. Samples were analyzed by CE to establish percent dephosphorylation and to determine if fluorescent peaks in addition to the intact phosphorylated and nonphosphorylated peptide appeared on the electropherograms. Dephosphorylation rates were reported as nmol peptide per minute per mg total cell protein (nmol min^{-1} mg^{-1}). For inhibition experiments, dose response curves were generated over a range of inhibitor concentrations and IC50 values were interpolated by regression of the linear portion of the semi-log plot of percent inhibition versus log_{10} of inhibitor concentration.

Single Cell Phosphatase Measurement. A431 cells were grown in DMEM on cell chambers comprising a round 25 mm diameter No. 1 glass coverslip bonded to a silicone O-ring (18 mm internal diameter) with PDMS. Pretreatment of cells, if any, was performed by removing media from a cell chamber, rinsing twice with 37 ^{0}C serum-free DMEM and then adding the appropriate inhibitor dissolved in serum-free DMEM and incubating at 37 ^{0}C for 10-20 min. After pretreatment, a cell chamber was placed on the microscope stage of the customized single-cell CE system,[21] a cell was visualized and microinjected with a mixture of peptide reporter and internal standard using a Transjector 5246 microinjection system (Eppendorf AG, Hamburg, Germany). The cell chamber temperature was maintained at 37 ^{0}C using a constant flow of warmed extracellular buffer (ECB; 10 mM HEPES, 135 mM NaCl, 5 mM KCl, 1 mM $CaCl_2$, 1 mM $MgCl_2$, pH 7.4) during microinjection, reporter

incubation, and cell lysis. At 60 s post-microinjection, the cell was lysed with a 532 nm ND:YAG pulsed laser[22] and electrokinetically injected into the capillary by applying a negative potential to the capillary outlet reservoir (5 s at 79 V/cm). The capillary inlet was then repositioned into a reservoir of electrophoretic buffer (140 mM borate, 150 mM SDS, 50 mM NaCl, pH 7.0), electrophoresis was performed (263 V/cm), and data was analyzed using Matlab and Origin. Data from untreated and inhibitor treated cells was compared using bootstrapping[23] and p-values were reported.

Statistical Analysis. The distribution of the difference between the mean %pTS13 remaining in each treatment group and the control group was calculated using bootstrapping. 10,000 bootstrap replicates were sampled (with replacement) from each group and the means of each bootstrap replicate were calculated. The distribution of the mean differences was estimated by the distribution of the differences between the appropriate pairs of bootstrap replicates. 95% confidence intervals for each difference were estimated using the bias-corrected and accelerated (BCa) method. The p-value for testing the null hypothesis of no difference in mean between each treatment group and the control group was estimated by dividing the number of bootstrap differences 0 or less by the total number of bootstrap replicates (i.e. 10,000).

Results and Discussion

Peptide Selection and Separation. In order to measure PTP activity in single cells, a phosphotyrosine-containing peptide reporter sequence (Glu-Glu-Leu-Glu-Asp-Asp-pTyr-Glu-Asp-Asp-Nle-Glu-Glu-amide, where Nle is norleucine) was chosen. The sequence was adapted from a peptide substrate of epidermal growth factor receptor (EGFR),[24] a receptor

tyrosine kinase opposed by phosphatases including PTPN1, PTPN2, SHP-1, and Cdc25A.[25-26] 6-FAM was conjugated to the N-terminus to permit fluorescence detection. Since incubation of peptides in cells or cell lysates can result in their metabolism by peptidases with cleavage at any peptide bond, the ability to electrophoretically separate pTS13, TS13 and their fluorescent fragments which are similar in charge/mass was critical for use of pTS13 as a reporter in cell lysates and single cells. Moreover it was critical that the sample matrix used for the separation be that of a physiologic buffer since the ultimate goal of this work was measurement of single-cell, reporter dephosphorylation during toxin exposure.

Initial methods development focused on the separation of pTS13 and TS13. A survey of separation buffers previously reported for peptides and highly negative analytes comprised borate with and without sodium dodecyl sulfate (SDS) or cetyltrimethlammonium bromide (CTAB), sodium citrate, sodium phosphate with SDS, tris(hydroxymethyl)aminomethane (Tris), and 1,1-bis(hydroxymethyl)ethyl)glycine (Tricine).[27] The best resolution observed during this screening was 1.3 ± 0.1 for 140 mM borate, 70 mM SDS, pH 7.5. This concentration of SDS is well above its critical micelle concentration (7.9-8.3 mM)[28] and thus the mode of separation was expected to be micellar electrokinetic capillary chromatography, modified by borate complexation. For both lysate and single-cell analyses, the sample matrix was not the electrophoretic buffer but a high-salt biocompatible buffer. When pTS13 and TS13 were loaded into the capillary using a high-salt, neutral-pH buffer (ECB) as the sample matrix, the peaks were no longer resolved (Figure 2.1a). The loss in separation capacity was most likely due to destacking of the analytes in the high ionic strength sample matrix. To minimize destacking when using high salt samples, 50 mM sodium chloride was added to the electrophoretic buffer to more closely match the ionic strength of the sample matrix i.e.

physiologic buffer, and SDS concentration was increased to 150 mM to increase micellar sweeping effects. Although the added salt minimized destacking, it resulted in a greatly increased current flow through the capillary necessitating electrophoretic separations at very low field strengths (≤ 160 V/cm) and consequent long separation times (1680 ± 54 s for TS13, 1760 ± 63 s for pTS13). For this reason, all subsequent separations were performed in a 30 μM ID capillary to maintain acceptable field strengths (260 V/cm) at low currents and shorter separation times (1170 ± 22 s for TS13, 1230 ± 26 s for pTS13). These conditions yielded separation of pTS13 and TS13 with a resolution of 3.4 ± 0.1, and efficiencies of 7.3 ± 0.6 x 10^4 (TS13) and 6.7 ± 0.5 x 10^4 (pTS13) theoretical plates (Figure 2.1b). Importantly, the ratio of the peak areas of pTS13 and TS13 to that of the total peptide was highly reproducible with an RSD of 0.032 and 0.023, respectively. Although these efficiencies are lower than for many peptide separations by CE, the highly negative analytes and high-salt sample matrix make this a challenging separation. Most important, the resolution was sufficient for the intended biological

application. The limit of detection for pTS13, defined as the smallest amount of analyte detectable with a signal-to-noise ratio greater than 3, was determined to be 4.4 x 10^{-20} mol.

The phospho- and nonphospho-peptides migrated 60 s apart; however, this spacing was not sufficient to consistently identify single peaks given the variability in the migration time especially in the presence of potentially biofouling constituents such as protein or cell debris. For this reason, 6-FAM was used as an internal standard for all biologic samples. This dye is detectable by LIF and migrates near TS13 and pTS13. The 12 possible fluorescent fragments generated by removal of C-terminal residues from TS13 were synthesized. Separation of all analytes simultaneously (Figure 2.1c) demonstrated that no

fragments co-migrated with 6-FAM, pTS13, or TS13, and thus any degradation of the reporter within the biologic sample will produce additional CE peaks.

Kinetics of *in vitro* Dephosphorylation. The human enzymes PTPN1 (PTP-1B) and PTPN2 (TC-PTP) favor substrates with acidic side-chains proximal to the phosphotyrosine residue, and are implicated in airway inflammation.[29-31] To determine if phosphatase activity could be measured using pTS13, the reporter at varying concentrations was incubated with recombinant PTPN1 and PTPN2. Product formation was quantified by CE and the percent dephosphorylated peptide was calculated as the ratio of the integrated area of the TS13 peak to the combined area of the pTS13 and TS13 peaks. The Michaelis constant (K_M), maximal reaction velocity (V_{max}), and turnover number (k_{cat}) were determined for pTS13 dephosphorylation by PTPN1 and PTPN2 (Table 2.1) by fitting the initial rates of product formation to the Michaelis-Menten equation. PTPN1 and PTPN2 showed first order kinetics with respect to pTS13 dephosphorylation. Previous studies of peptide substrates for PTPN1 have reported K_M values of 2.6-23 μM, with k_{cat} values of 55.7-78.9 s^{-1},[32-33] comparable to the values observed for pTS13. The kinetics of PTPN2 are less well documented, but a K_M for phosphotyrosine was measured to be 300 μM,[34] which is approximately 1000-fold higher than that seen for pTS13. This is consistent with previous studies comparing PTP dephosphorylation for peptide substrates and phosphotyrosine alone.[33] In summary, Michaelis-Menten kinetics measured with recombinant phosphatases and pTS13 are consistent with the existing literature, establishing the utility of this method for studying PTP activity *in vitro*.

Inhibition of Recombinant Enzymes by Toxins From Diesel Exhaust. Inhibitors of PTP activity were chosen to represent three major mechanisms of environmentally

relevant PTP inhibition: active site cysteine oxidation, covalent modification, and non-oxidative inhibition by transition metals.[35] Vanadium is a heavy metal found in fossil fuels and is released during combustion.[36] Several oxidation states of vanadium are established PTP inhibitors, including pervanadate, which acts through direct oxidation of the catalytic cysteine.[37] The polycyclic aromatic hydrocarbon 1,2-naphthoquinone is a naphthalene derivative generated by diesel combustion and petroleum processing which covalently and irreversibly arylates cysteine and histidine residues in the PTP active site.[7] Finally, zinc is a major transition metal component of diesel exhaust particles that is theorized to inhibit PTP action by a non-redox mechanism involving direct interaction with vital active site residues.[38]

To establish whether PTP inhibition could be measured using our phosphatase activity reporter, pTS13 was incubated with recombinant PTPN1 and PTPN2 in the presence of the aforementioned inhibitors across a range of concentrations. The enzyme was pretreated with sodium pervanadate, 1,2-naphthoquinone, or Zn^{2+}, then pTS13 dephosphorylation was assessed by CE. Dose-response curves were generated (Figure 2.2) to establish this system as a useful method for measurement of PTP inhibition *in vitro*. For PTPN1 inhibition, IC50 values for 1,2-naphthoquinone, pervanadate and Zn^{2+} were determined as 520 nM, 59 nM, and 28 μM respectively. IC50 values for these compounds with PTPN2 were found to be 53 nM, 39 nM, and 87 μM. These data are similar to previous reports of PTPN1 inhibition with 1,2-naphthoquinone (IC_{50}: 1.6-5 μM),[7, 39] pervanadate (IC_{50}: 400 nM),[37] and PTPN2 inhibition with Zn^{2+} (85% inhibition at 100 μM).[40] All three of these agents inhibit PTPs through complex and often overlapping mechanisms. While Zn^{2+} is thought to bind directly to the PTP active site, it is also implicated in oxidative inhibition. Pervanadate solutions exist as a mixture of vanadium oxidation states and contain

H2O2, itself an oxidative inhibitor of PTP activity. Finally, 1,2-naphthoquinone irreversibly arylates the catalytic cysteine of PTPs, but also arylates other cysteine and histidine residues, which likely underlies the difference in inhibition between PTPN1 and PTPN2 for this agent. The complex mechanisms of inhibition exhibited by these environmental agents is also likely to be the basis for the variable shapes observed for dose-response curves generated for these PTP inhibitors.

Lifetime of pTS13/TS13 in Cell Lysates. To assess reporter susceptibility to intracellular degradation, TS13 was incubated with A431 cell lysates and samples were analyzed by CE. One additional peak appeared over 3 hours. This breakdown product was identified as the 8 residue fragment (6FAM-EELEDDYE-COOH) based on co-migration with the synthetic fragment. The average rate of formation, and thus reporter breakdown, was 100 ± 8.2 fmol min^{-1} mg^{-1}. This rate is approximately 10^4 times slower than the dephosphorylation rate measured in A431 lysates (discussed below), suggesting that TS13 is sufficiently robust to degradation for its intended applications. Several peptides have been shown to undergo rapid degradation in cell lysates at rates ranging from 1.4-13 nmol min^{-1} mg^{-1},[41-42] approximately 10^4-10^5 fold faster than observed for TS13. The peptidase resistance of TS13 is consistent with the finding that both glutamic and aspartic acid, the two most prevalent residues in this reporter, are moieties not preferred by peptidases.[42]

PTP activity and Inhibition in A431 Cell Lysates. Unlike an isolated recombinant enzyme, cellular PTP activity is opposed by tyrosine kinases. To determine if PTP activity could be measured in the context of cellular contents, pTS13 was incubated with whole cell lysates generated from A431 epidermoid carcinoma cells with and without the previously described environmental toxins (Figure 2.3). In the absence of inhibitors, pTS13

dephosphorylation occurred at a rate of 1.4 ± 0.3 nmol min^{-1} mg^{-1}. Toxin inhibition of total PTP activity in A431 lysates was similar to that seen in recombinant PTPs, with IC50 values of 470 nM, 100 nM, and 35 μM for 1,2-naphthoquinone, pervanadate, and Zn^{2+} respectively. These values are comparable to those seen for recombinant PTPs, and agree with previously reported C6 cell lysate inhibition by Zn^{2+} (IC_{50}: 31 μM).[38]

Lifetime of pTS13/TS13 in Single Cells. The degradation resistance of the PTP reporter in living cells was tested by microinjection of single A431 cells with TS13 and single-cell analysis by CE. A single degradation product was observed and corresponded to the 8 residue fragment based on migration relative to TS13. This suggests that degradation patterns for TS13 in intact A431 cells and lysates are similar. The degradation rate was linearly correlated (R^2 = 0.8) with amount of TS13 injected, suggesting first-order kinetics. The amount of peptide delivered ranged from 0.2-35 amol and the median degradation rate was 39 fmol min^{-1} mg^{-1} with first and third quartiles (Q_1 and Q_3) of 22 and 440 fmol min^{-1} mg^{-1}, similar to the rate observed in A431 cell lysates. The median half-life for TS13 was 35 min (Q_1 = 23 min, Q_3 = 39 min), approximately 250-fold longer than a previous report for a native peptide in living cells.[43]

Single A431 Cell PTP Activity. Cell lysates lack the organization and compartmentalization of the intact cell and represent the pooled average of all processes occurring within a population, obscuring any intercellular heterogeneity. To demonstrate the utility of pTS13 as a reporter of enzyme activity in single cells, individual A431 cells were analyzed with and without pretreatment with environmental toxins (Figure 2.4). In untreated cells, a median of 0% (Q1 = 0%, Q3 = 11%) remaining phosphorylation was observed after 60 s. For the majority of these cells, 100% dephosphorylation had occurred within this time

frame, so rates could not be calculated. A lower limit to the rate was estimated by assuming a total protein concentration of 1 g/mL and a 500 fL cell volume[44] for the average mammalian cell. The median rate was 2.1 pmol min^{-1} mg^{-1} (Q_1 and Q_3 of 1.1 and 8.0 pmol min^{-1} mg^{-1}), significantly lower than seen in lysates, however this difference is overestimated by the inability to calculate exact rates for single cells, *i.e.* if 100% dephosphorylation is achieved in less than 60 s, actual rates will be higher than those calculated. Compartmentalization of PTPs within the intact architecture of living cells could also contribute to lower dephosphorylation rates in single cells. Plots of percent dephosphorylation *vs.* amount of peptide delivered showed that across the mass range observed (0.5-33 amol), PTP activity was not saturated. Treatment of A431 cells with sodium pervanadate (1 mM) prior to microinjection resulted in a median of 53% (Q_1 = 36%, Q_3 = 77%) phosphorylation remaining in 60 s. Results of 1,2-naphthoquinone (50 μM) and zinc pyrithione (100 μM) pretreatment were similar, yielding 41% (Q_1 = 0%, Q_3 = 96%) and 50% (Q_1 = 46%, Q_3 = 74%) median phosphorylation remaining after 60 s, respectively. Comparison of dephosphorylation for each treatment group versus untreated controls found statistically significant inhibition with p-values of 0.035, 0.0072, and 0.002 for 1,2-napthoquinone, zinc pyrithione, and pervanadate. The measurement of the relative peak area of pTS13 to that of total peptide peak area in the presence of a lysed single cell was highly reproducible (RSD = 0.018). Prior work has shown that the termination of intracellular reactions by laser lysis[45] and the introduction of cell contents into the capillary by electrokinetic injection[22] are highly reproducible. Thus the most likely source of the measured variability in the PTP activity is the cellular heterogeneity in signaling.

The concentrations of 1,2-naphthoquinone and pervanadate necessary to ellicit 50% inhibition of PTP activity in single cells are 3 orders of magnitude higher than for lysates, while there is little difference seen for zinc pyrithione. Although the ionophore pyrithione aids entry of Zn^{2+} into cells, pervanadate has no such ionophore or any established membrane transporter, potentially limiting its access to the cytoplasm. 1,2-naphthoquinone is highly lipophilic and may partition extensively in the cell membrane. Additionally, unlike for Zn^{2+}, inhibition of PTPs by pervanadate requires oxidation, and the antioxidative machinery of intact cells has not been diluted or disorganized as is the case in a lysate. Exposure of intact cells to these toxins clearly inhibits PTP activity, and the variability between cells observed in these studies is consistent with previous reports of phenotypic heterogeneity in clonal populations,[46] underlining the value of single-cell measurements as compared to bulk analysis of many cells.

Conclusion

A novel chemical cytometry approach to measure PTP activity was demonstrated for analysis of recombinant enzymes *in vitro*, cell lysates, and single cells. In each system, total PTP activity was assessed by measuring dephosphorylation of a fluorescent substrate peptide. Inhibition of PTP activity by environmental toxins was observed for recombinant enzymes and lysates at levels similar to those previously reported. In single A431 cells, pretreatment with all toxins reduced PTP activity relative to untreated cells, with substantial variation between cells. This heterogeneity seen in cultured cells illustrates the value of analyzing individual cells rather than population averages. It should also be noted that relative to A431 lysates, the inhibition of PTP activity in single A431 cells required much higher

concentrations of inhibitors. The potential challenges to inhibitors, particularly pervanadate and 1,2-napthoquinone entering intact cells and therefore being less accessible to PTPs than would be the case in lysates has been discussed. Additionally, intact cells possess highly effective mechanisms for limiting oxidative stress that are likely to be disrupted upon cell lysis. Finally, as discussed in Chapter 1, PTP substrate recognition and activity depends on a complex network of interactions often involving protein-protein interactions in addition to the PTP itself. Because an intact cell maintains its physiological architecture while cell lysis disrupts this natural organization, it is unsurprising that the PTP behavior of an intact cell would differ from that of a lysate.

This approach provides several advantages over existing techniques. The simplicity of sample preparation and assay protocols makes this technique an attractive option for analysis of recombinant enzymes and cell lysates, and the high sensitivity and flexibility is well suited to analysis of intact single cells. This system does not require genetic manipulation of cells, making it useful for analysis of primary cells. While microinjection was utilized in these studies to deliver reporter into intact cells, a variety of alternative delivery methods exist, including conjugation of cell penetrating peptides or lipids and liposome-based approaches. Optimal reporter delivery conditions should afford efficient and reliable loading of intact cells while minimizing cellular stress response to avoid undue perturbation of signaling. The ability to pre-select individual cells using microscopy permits analysis of desired subpopulations of viable cells in low viability or highly complex samples as well as very small samples. These characteristics in particular suggest this technique will be valuable in the analysis of specimens such as airway brush biopsies and tumor samples. Additionally, enzyme activity is measured directly without the need for antibodies which,

combined with the analytical separation and tunability of a peptide substrate reporter, allows for simultaneous multiplexed measurements of several signaling events and provides a valuable complement to approaches focusing on genetics or protein expression. While the specificity of pTS13 has not been investigated to date, characterizing which PTPs most efficiently dephosphorylate this reporter would provide more detail to the experimental readout and serve as a basis for potential structural refinements to tailor specificity to an intended target or group of targets. In addition to refinement of the substrate sequence, the inclusion of targeting moieties such as nuclear localization signals or lipids could provide insight into PTP activity in the context of subcellular localization, an important aspect of PTP regulation. In conclusion, the ability to analyze the effects of extracellular insults on signaling in small, heterogeneous samples of primary cells using a sensitive and flexible reporter promises to be a valuable new research tool in environmental health research in particular as well as the larger field of cell signaling.

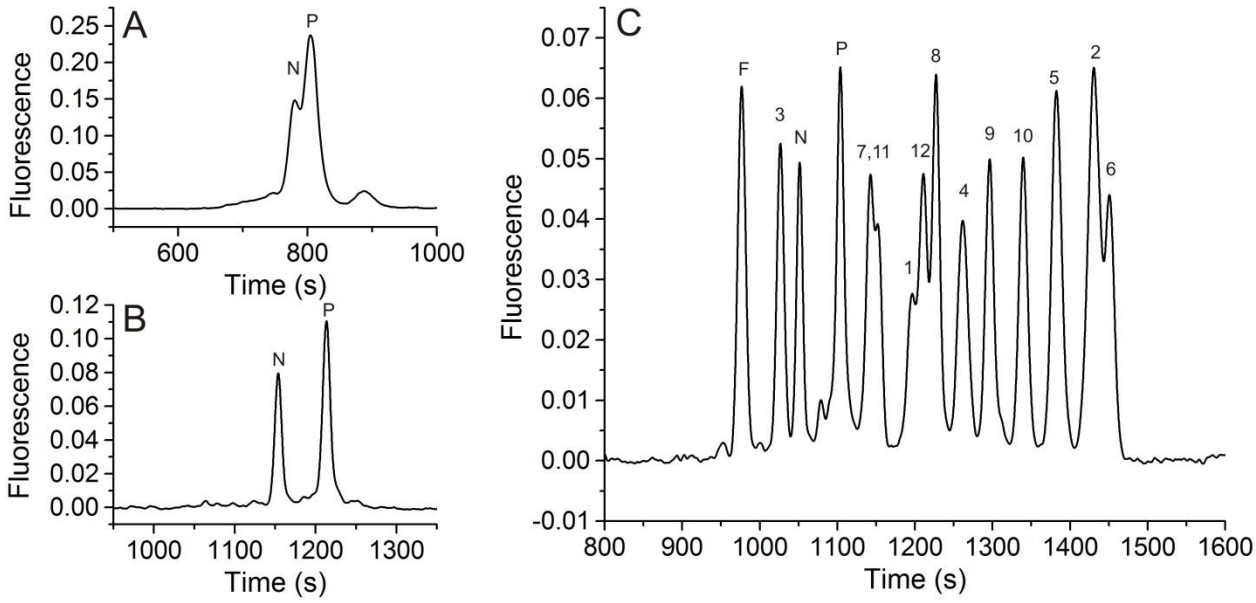

Figure 2.1. Separation of pTS13 (P) and TS13 (N) in 140 mM borate, 70 mM SDS, pH 7.4 in a 50-μm diameter capillary (A) or with 140 mM borate, 150 mM SDS, 50 mM NaCl, pH 7.4 in a 30-μm diameter capillary (B). Reporter species were also separated from all fluorescent fragments (C), indicated by length in residues (*e.g.* fragment 1 is 6-FAM-Glu-COOH), as well as from the 6-FAM internal standard (F).

Enzyme	K_M (nM)	V_{max} (nM s^{-1} ng^{-1})	k_{cat} (s^{-1})
PTPN1	770 ± 250	2.2 ± 0.25	21 ± 2.4
PTPN2	290 ± 54	3.1 ± 0.18	30 ± 1.7

Table 2.1. Kinetic constants K_M and V_{max} for pTS13 dephosphorylation by recombinant PTPN1 and PTPN2 were determined by fitting the Michaelis-Menten equation to initial reaction rates obtained over a range of substrate concentrations. K_{cat} was calculated as V_{max}/[E] where [E] is enzyme concentration.

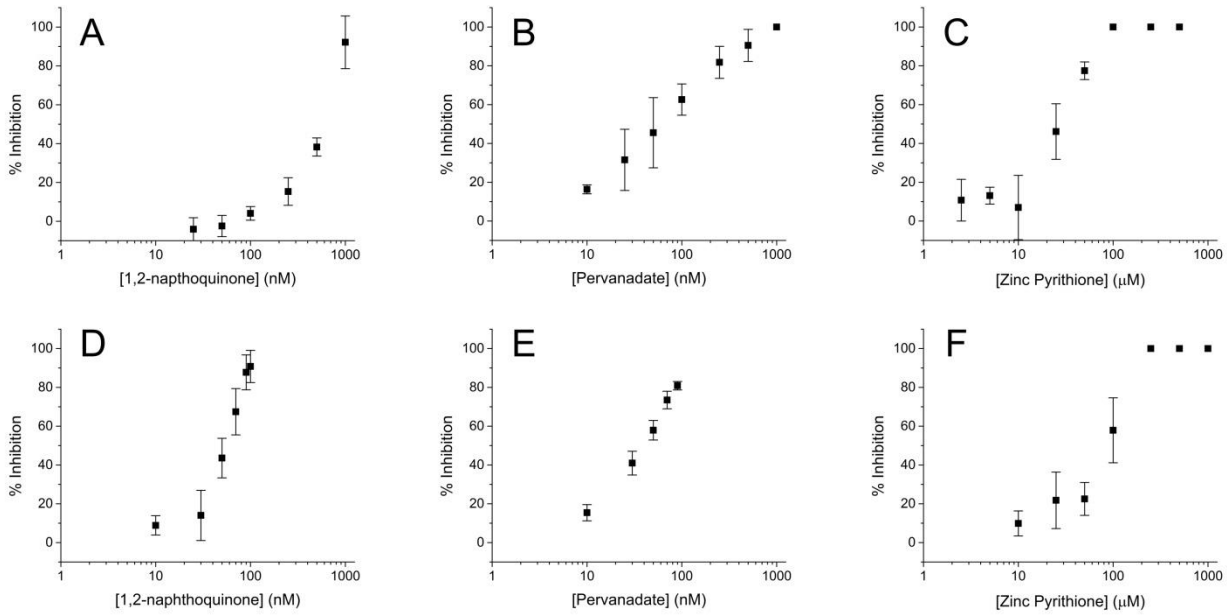

Figure 2.2. (A-C) Recombinant PTPN1 and (D-F) PTPN2 were pretreated with a range of inhibitor concentrations for 10 min and then incubated with pTS13 for 10 min. Percent inhibition was calculated relative to the dephosphorylation observed in the absence of inhibitor. Error bars represent the standard deviation of three replicates (n = 3).

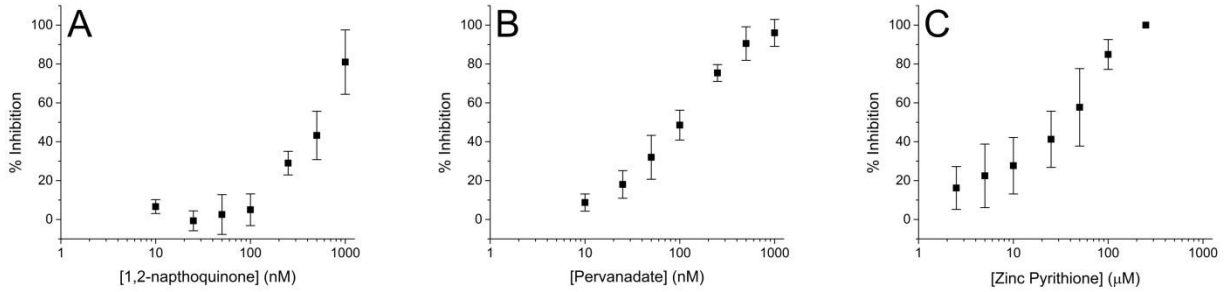

Figure 2.3. (A-C) A431 cell lysates (10 μg total protein) were pretreated with a range of inhibitor concentrations for 10 min and then incubated with pTS13 for 90 s. Percent inhibition was calculated relative to the dephosphorylation observed in the absence of inhibitor. Error bars represent the standard deviation of three replicates (n = 3).

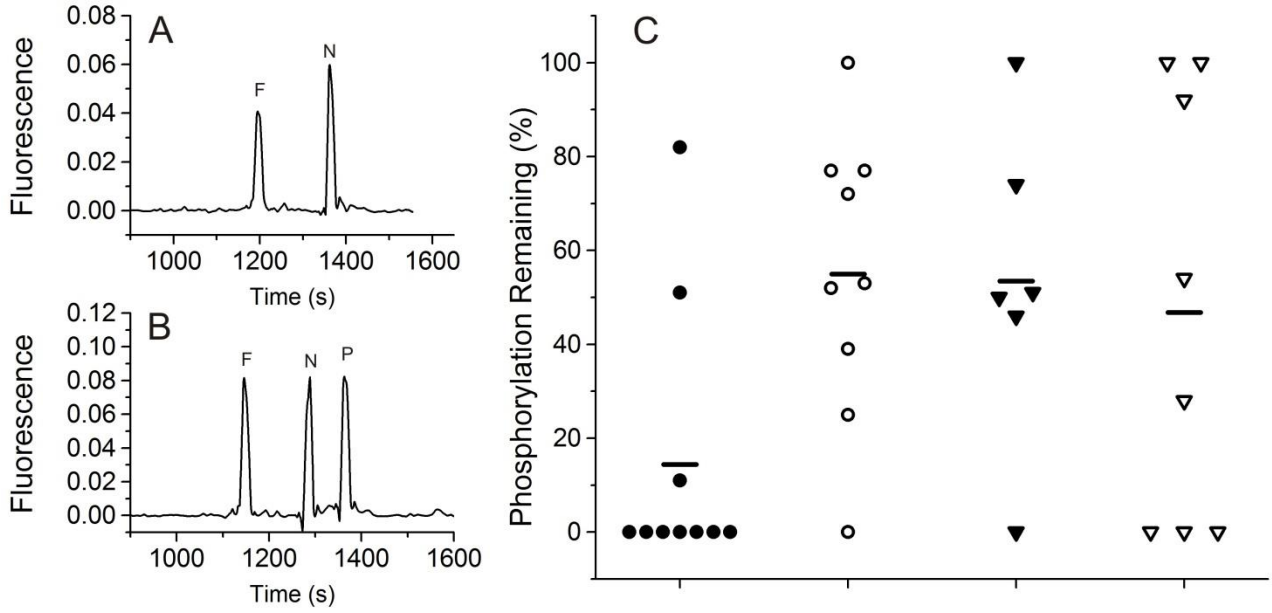

Figure 2.4. Single A431 cells were incubated in serum-free medium with and without inhibitors for 10 min, microinjected with pTS13, and analyzed by CE after 60 s incubation. Representative electropherograms of (A) full dephosphorylation in an untreated cell and (B) partial dephosphorylation in a pervanadate treated cell. (C) Summary of PTP inhibition seen after treatment with (•) no inhibitor, (◦) 1 mM sodium pervanadate, (▼)100 μM zinc pyrithione , or (▽) 50 μM 1,2-naphthoquinone. Each marker represents a single cell while bars represent the mean for each group.

References

1. Vang, T.; Miletic, A. V.; Arimura, Y.; Tautz, L.; Rickert, R. C.; Mustelin, T., *Annu Rev Immunol,* **2008,** *26,* 29-55.

2. Mustelin, T., *Adv Exp Med Biol,* **2006,** *584,* 53-72.

3. Tal, T. L.; Bromberg, P. A.; Kim, Y.; Samet, J. M., *Toxicol Appl Pharmacol,* **2008,** *233,* 382-388.

4. Miller, M. R.; Shaw, C. A.; Langrish, J. P., *Future Cardiol,* **2012,** *8,* 577-602.

5. U.S. EPA. Integrated Science Assessment for Particulate Matter (Final Report). 2009.

6. Gurgueira, S. A.; Lawrence, J.; Coull, B.; Murthy, G. G.; Gonzalez-Flecha, B., *Environ Health Perspect,* **2002,** *110,* 749-755.

7. Iwamoto, N.; Sumi, D.; Ishii, T.; Uchida, K.; Cho, A. K.; Froines, J. R.; Kumagai, Y., *J Biol Chem,* **2007,** *282,* 33396-33404.

8. Gaur, D.; Thapliyal, N.; Kishore, S.; Pathak, V., *Efficacy of broncho-alveolar lavage and bronchial brush cytology in diagnosing lung cancers*. 2007; Vol. 24, p 73-77.

9. Romagnoli, M.; Vachier, I.; Vignola, A. M.; Godard, P.; Bousquet, J.; Chanez, P., *Respir Med,* **1999,** *93,* 461-466.

10. Yendamuri, S.; Vaporciyan, A. A.; Zaidi, T.; Feng, L.; Fernandez, R.; Bekele, N. B.; Hofstetter, W. L.; Jiang, F.; Mehran, R. J.; Rice, D. C.; Spitz, M. R.; Swisher, S. G.; Walsh, G. L.; Roth, J. A.; Katz, R. L., *J Thorac Oncol,* **2008,** *3,* 979-984.

11. Yang, I. V.; Tomfohr, J.; Singh, J.; Foss, C. M.; Marshall, H. E.; Que, L. G.; McElvania-Tekippe, E.; Florence, S.; Sundy, J. S.; Schwartz, D. A., *Am J Respir Crit Care Med,* **2012,** *185,* 620-627.

12. Bewig, B.; Haacke, T. C.; Tiroke, A.; Bastian, A.; Bottcher, H.; Hirt, S. W.; Rautenberg, P.; Haverich, A., *Respiration,* **2000,** *67,* 166-172.

13. Lu, C., *Chemical cytometry : ultrasensitive analysis of single cells*. Wiley-VCH: Weinheim, 2010; p xix, 247 p.

14. Kovarik, M. L.; Allbritton, N. L., *Trends Biotechnol,* **2011,** *29,* 222-230.

15. Lin, Y.; Trouillon, R.; Safina, G.; Ewing, A. G., *Anal Chem,* **2011,** *83,* 4369-4392.

16. Piccard, H.; Hu, J.; Fiten, P.; Proost, P.; Martens, E.; Van den Steen, P. E.; Van Damme, J.; Opdenakker, G., *Electrophoresis,* **2009,** *30,* 2366-2377.

17. Keithley, R. B.; Rosenthal, A. S.; Essaka, D. C.; Tanaka, H.; Yoshimura, Y.; Palcic, M. M.; Hindsgaul, O.; Dovichi, N. J., *Analyst,* **2013,** *138,* 164-170.

18. Phillips, R. M.; Blair, E.; Lawrence, D. S.; Sims, C. E.; Allbritton, N. L., *Anal Chem,* **2013**.

19. Masui, H.; Castro, L.; Mendelsohn, J., *J Cell Biol,* **1993,** *120,* 85-93.

20. Proctor, A.; Wang, Q.; Lawrence, D. S.; Allbritton, N. L., *Analyst,* **2012,** *137,* 3028-3038.

21. Nelson, A. R.; Allbritton, N. L.; Sims, C. E., *Methods Cell Biol,* **2007,** *82,* 709-722.

22. Sims, C. E.; Meredith, G. D.; Krasieva, T. B.; Berns, M. W.; Tromberg, B. J.; Allbritton, N. L., *Anal Chem,* **1998,** *70,* 4570-4577.

23. Efron, B.; Tibshirani, R., *An introduction to the bootstrap*. Chapman & Hall: New York, 1993; p xvi, 436 p.

24. Guyer, C. A.; Woltjer, R. L.; Coker, K. J.; Staros, J. V., *Arch Biochem Biophys,* **1994,** *312,* 573-578.

25. Wang, Z.; Wang, M.; Lazo, J. S.; Carr, B. I., *J Biol Chem,* **2002,** *277,* 19470-19475.

26. Tiganis, T., *IUBMB Life,* **2002,** *53,* 3-14.

27. Weinberger, R., *Practical capillary electrophoresis*. 2nd ed.; Academic Press: San diego, CA, 2000; p xvii, 462 p.

28. Perez-Rodriguez, M.; Prieto, G.; Rega, C.; Varela, L. M.; Sarmiento, F.; Mosquera, V., *Langmuir,* **1998,** *14,* 4422-4426.

29. Human Protein Reference Database. http://www.hprd.org/PhosphoMotif_finder (accessed July 17, 2012).

30. Jia, Z.; Barford, D.; Flint, A. J.; Tonks, N. K., *Science,* **1995,** *268,* 1754-1758.

31. Pouliot, P.; Bergeron, S.; Marette, A.; Olivier, M., *Immunology,* **2009,** *128,* 534-542.

32. Salmeen, A.; Andersen, J. N.; Myers, M. P.; Tonks, N. K.; Barford, D., *Mol Cell,* **2000,** *6,* 1401-1412.

33. Zhang, Z. Y.; Walsh, A. B.; Wu, L.; McNamara, D. J.; Dobrusin, E. M.; Miller, W. T., *J Biol Chem,* **1996,** *271,* 5386-5392.

34. Zhao, Z.; Zander, N. F.; Malencik, D. A.; Anderson, S. R.; Fischer, E. H., *Anal Biochem,* **1992,** *202,* 361-366.

35. Samet, J. M.; Tal, T. L., *Annu Rev Pharmacol Toxicol,* **2010,** *50,* 215-235.

36. Chen, F.; Shi, X., *Environ Health Perspect,* **2002,** *110 Suppl 5,* 807-811.

37. Huyer, G.; Liu, S.; Kelly, J.; Moffat, J.; Payette, P.; Kennedy, B.; Tsaprailis, G.; Gresser, M. J.; Ramachandran, C., *J Biol Chem,* **1997,** *272,* 843-851.

38. Haase, H.; Maret, W., *Exp Cell Res,* **2003,** *291,* 289-298.

39. Ahn, J. H.; Cho, S. Y.; Ha, J. D.; Chu, S. Y.; Jung, S. H.; Jung, Y. S.; Baek, J. Y.; Choi, I. K.; Shin, E. Y.; Kang, S. K.; Kim, S. S.; Cheon, H. G.; Yang, S. D.; Choi, J. K., *Bioorg Med Chem Lett,* **2002,** *12,* 1941-1946.

40. Zander, N. F.; Lorenzen, J. A.; Cool, D. E.; Tonks, N. K.; Daum, G.; Krebs, E. G.; Fischer, E. H., *Biochemistry,* **1991,** *30,* 6964-6970.

41. Mo, X. Y.; Cascio, P.; Lemerise, K.; Goldberg, A. L.; Rock, K., *J Immunol,* **1999,** *163,* 5851-5859.

42. Beninga, J.; Rock, K. L.; Goldberg, A. L., *J Biol Chem,* **1998,** *273,* 18734-18742.

43. Reits, E.; Griekspoor, A.; Neijssen, J.; Groothuis, T.; Jalink, K.; van Veelen, P.; Janssen, H.; Calafat, J.; Drijfhout, J. W.; Neefjes, J., *Immunity,* **2003,** *18,* 97-108.

44. Schmid, A.; Kortmann, H.; Dittrich, P. S.; Blank, L. M., *Curr Opin Biotechnol,* **2010,** *21,* 12-20.

45. Li, H.; Sims, C. E.; Wu, H. Y.; Allbritton, N. L., *Anal Chem,* **2001,** *73,* 4625-4631.

46. Stockholm, D.; Benchaouir, R.; Picot, J.; Rameau, P.; Neildez, T. M.; Landini, G.; Laplace-Builhe, C.; Paldi, A., *PLoS One,* **2007,** *2,* e394.

III. Analysis of Protein Tyrosine Phosphatase Activity in Single Human Airway Cells *ex vivo* by Chemical Cytometry

Overview

Protein tyrosine phosphatase (PTP) activity and inhibition in single human airway epithelial cells (hAECs) was measured using a capillary electrophoresis-based assay. A fluorescent phosphopeptide PTP substrate was microinjected into single BEAS-2B immortalized bronchial epithelial cells and rapid dephosphorylation at a rate greater than 2.2 pmol min^{-1} mg^{-1} was observed. Pretreatment of the cells with the known PTP inhibitors pervanadate, Zn^{2+}, and 1,2-naphthoquinone resulted in 76%, 69%, 100% median inhibition of PTP activity, respectively. Reporter proteolysis in single BEAS-2B cells occurred at a median rate of 43 fmol min^{-1} mg^{-1} resulting in a median half-life of 20 min. These studies were then extended to primary hAECs cultured from bronchial brushings of living human subjects. The reporter displayed a similar median half-life of 28 min in these single primary cells. Dephosphorylation of the reporter occurred at rates greater than 2.2 pmol min^{-1} mg^{-1}, and pre-incubation of the cells with the inhibitors pervanadate, Zn^{2+}, and 1,2-naphthoquinone yielded 91%, 88%, and 87% median PTP inhibition, respectively. Finally, single viable epithelial cells (n=3) were identified from a bronchial brushing specimen by positive immunostaining for the epithelial cell adhesion molecule (EpCAM) and absence of propidium iodide staining. Dephosphorylation rates ranging from 0.35-36 pmol min^{-1} mg^{-1}

were observed using capillary electrophoresis, demonstrating direct applicability of this technique for quantification of PTP activity in small, heterogeneous samples of primary cells.

Introduction

Cardiovascular disease is the leading cause of death in the US for both men and women, resulting in 25% of deaths in 2008.[1] Inhalation of fine and ultrafine particulate matter (PM) generated by the combustion of diesel fuel is linked to increased blood pressure,[2] decreased cardiac autonomic control,[3] and significantly increased risk of heart attack and stroke.[4] *In vitro* studies have demonstrated that inhaled PM leads to increased inflammatory signaling in airway cells[5-7] and suggest that inhibition of protein tyrosine phosphatases (PTPs) plays a prominent role in this process.[8-9] Immortalized airway cell lines and cultured primary airway epithelia are valuable model systems for these studies, but fail to fully recapitulate the phenotype of cells in the intact airway.[10] Analysis of fresh airway epithelia, obtained through bronchial brushing, from human subjects exposed to well-characterized PM would provide a more physiological context for studies of PM inhalation and its effects on airway signaling. However, analysis of these *ex vivo* specimens is technically challenging due to the very small sample sizes (on average 10^5 total cells) with cell viabilities of 11-33%. These samples are also composed of a mixed cell types with immune and squamous cells comprising 2-44% of the cells.[11]

Previous analyses of epithelial cells from bronchial brushing specimens have utilized a variety of analytical methods although most studies have employed genetic approaches due to the readily available amplification methods for nucleotide analyses. Fluorescence in situ hybridization (FISH)[12] and polymerase chain reaction (PCR)[13] have been used, respectively,

to detect chromosomal abnormalities and viral DNA in bronchial brushings. RNA microarrays[14] have been used to probe for transcriptional changes associated with airway disease. Immunohistochemistry (IHC) using anti-phosphotyrosine antibodies has been employed to assess the presence of phosphoproteins in these samples as an indirect measure of PTP activity.[15] However, none of these approaches directly measure PTP activity in living cells.

Chemical cytometry, defined as the direct measurement of chemical processes at the single cell level, has the potential to be an important addition to techniques that characterize the genetic makeup and protein expression of bronchial brushing specimens. Among the many chemical cytometry approaches that have been described,[16-17] the use of capillary electrophoresis with laser-induced fluorescence (CE-LIF) is well-suited for addressing the challenges associated with bronchial brushings. Limits of detection approaching 10^{-21} mol for CE-LIF[18] permit the analysis of single cells and therefore size-limited samples. This provides two additional advantages when dealing with heterogeneous samples. Because information about each cell is acquired independently, variation between similar cells as well as between subpopulations is not lost due to population averaging.[16] Additionally, individual cells of interest can be readily selected from a mixed population by vital staining to assess viability or extracellular markers. Finally, using this approach enzyme activity can be measured directly without the need for genetic manipulation and is thus applicable to both immortalized and primary cells.[19] The advantages of chemical cytometry in single-cell analyses led to the recent development of a single-cell assay of PTP activity[20] using a fluorescent phosphopeptide PTP substrate termed “pTS13”. Initial validation for this

approach was performed in A431 epidermoid carcinoma cells, a well-established model system for the study of tyrosine phosphorylation dynamics.[21]

In the present work, we demonstrate the utility of a previously described fluorescent peptide reporter for quantification of PTP activity in single human airway cells, including epithelial cells from a fresh bronchial brushing specimen. Intracellular proteolysis of the peptide was assessed in single BEAS-2B cells using previously established capillary electrophoresis conditions capable of resolving the peptide from all fluorescent cleavage products. PTP activity was then quantified in single BEAS-2B cells, as well as the inhibition of PTP activity resulting from exposure to three environmental toxins. This approach was then extended to the analysis of single cultured primary human airway epithelial cells (hAECs), wherein reporter proteolysis, PTP activity, and PTP inhibition by toxins were quantified. Finally, single viable epithelial cells in a fresh bronchial brushing specimen were identified and PTP activity was assessed, demonstrating the direct applicability of this chemical cytometry method to the analysis of fresh *ex vivo* airway samples. Primary hAECs and bronchial brushings were obtained from Lisa A. Dailey and statistical analysis was performed by Eric Bair.

Experimental Section

Materials. BEAS-2B cells were obtained from ATCC and primary human airway epithelial cells (hAECs) and bronchial brushing specimens were obtained from the Human Studies Division of the National Health and Environmental Effect Research Laboratory (US Environmental Protection Agency, Chapel Hill, NC). Keratinocyte Basal Medium (KBM-Gold), Bronchial Epithelial Basal Medium (BEGM), and Singlequots™ growth factors, cytokines, and supplements were from Lonza. Sylgard 184 polydimethylsiloxane (PDMS)

was purchased from Dow Corning, antibodies from Biolegend, and fluorescence microscopy filter sets from Chroma. All other chemicals were purchased from either Sigma or Fisher.

Cell Culture. Wi-38 cells were grown in Dulbecco's Modified Eagle's Medium (DMEM) plus 10% fetal bovine serum (FBS). BEAS-2B cells were grown in Keritinocyte Growth Medium (KGM) prepared from KBM-Gold and a KGM-Gold Singlequots™ kit. Primary hAECs were grown in Bronchial Epithelial Growth Medium (BEGM) prepared from BEBM and a BEGM Singlequots™ kit. BEAS-2B cultures were propagated in 25 cm^2 tissue culture flasks and passaged when cells reached 60-80% confluency. Cells intended for single cell analysis were grown on cell chambers comprising a silicone O-ring attached to a round no. 1 glass coverslip (25 mm diameter) with PDMS. Cryopreserved hAECs (passage 3) were thawed and plated directly onto cell chambers. Cells from the *ex vivo* bronchial brushing specimen were grown in cell chambers in which a polystyrene coverslip replaced the glass coverslip.

Immunofluorescence. Cells in a chamber were rinsed with 37 °C extracellular buffer (ECB; 10 mM HEPES, 135 mM NaCl, 5 mM KCl, 1 mM $CaCl_2$, 1 mM $MgCl_2$, pH 7.4) to remove media. Excess ECB was aspirated and antibody solution (Alexafluor 647 anti-human C326 (EpCAM) diluted 1:40 in ECB) was added to the chamber and incubated for 15 min at 37 °C. Unbound antibody was then removed by rinsing the chamber with ECB. Propidium iodide solution (5 μg/mL in ECB) was then added to the chamber and cells were incubated for 5 min. Excess propidium iodide was removed by rinsing with ECB and cells were imaged at 25X magnification. Fluorescence images were obtained with xenon arc lamp illumination for detection of Alexafluor 647 (Cy5 filter set) and propidium iodide (Cy3 filter

set). Digital images were acquired and processed using Micro-Manager and ImageJ software.

Single cell capillary electrophoresis. Single cells grown in chambers were microinjected with the PTP reporter, pTS13, or its non-phosphorylated analogue, TS13, using a Transjector 5246 microinjection system (Eppendorf AG, Hamburg, Germany). Cells were kept at 37 °C under a flow of warm ECB until the desired time point was reached, whereupon the cell of interest was lysed with an Nd:YAG pulsed laser (532 nm). Cell contents were aspirated into the capillary by electrokinetic injection (5 s at 79 V/cm) and CE-LIF was performed at 263 V/cm on a customized system. CE separations were performed in 140 mM borate, 150 mM sodium dodecyl sulfate (SDS), 50 mM NaCl, pH 7.4. Fluorescence and current data were collected using Labview (National Instruments, Austin, TX) and analyzed with Matlab (The Mathworks, Natick, MA) and Origin (OriginLab, Northampton, MA) software.

Reporter lifetime measurement in single cells. BEAS-2B or cultured hAECs were microinjected with TS13 and analyzed by CE-LIF after 1.5-12 min. The amount of intact TS13 remaining was calculated as the corrected area of the TS13 peak by the sum of the corrected areas for all peaks. Data was analyzed using Excel (Microsoft) and Origin.

Single cell phosphatase activity assay. BEAS-2B, cultured hAE, and fresh primary human airway cells were microinjected with pTS13 and analyzed by CE-LIF after 60 s. For heterogeneous airway samples, epithelial cells were identified by anti-EpCAM vital staining prior to microinjection. Dephosphorylation was assessed by dividing the corrected area of the pTS13 peak by the combined corrected areas of pTS13 and TS13 peaks. Quantification

of TS13 and pTS13 was achieved by back-calculation from corrected peak area based on data from injection of known amounts of standard.

Statistical analysis. Comparisons of PTP inhibition for treated vs. control cells and across similarly treated cell lines was performed by bootstrapping as previously described.[20]

Results and Discussion

Lifetime of the PTP reporter in single BEAS-2B cells. BEAS-2B cells are immortalized, non-tumorigenic human bronchial epithelial cells commonly used in airway research owing to their ability to recapitulate many of the features of normal primary airway cells including antioxidative capacity, inflammatory response, and matrix attachment.[22-24] In order to accurately measure PTP activity in cells, the reporter must be robust to intracellular degradation. To assess reporter susceptibility to intracellular degradation in BEAS-2B cells, single cells were microinjected with non-phosphorylated pTS13, termed "TS13", and analyzed by CE-LIF. The median amount of TS13 introduced into a single cell was 0.69 amol (1 μM for a cell volume of 500 fL) with first and third quartiles (Q_1 and Q_3) of 0.21 and 0.83 amol (0.42 and 2.0 μM). The electrophoretic traces possessed a peak co-migrating with TS13 and a peak co-migrating with the 8-residue fragment (6FAM-Glu-Glu-Leu-Glu-Asp-Asp-Tyr-Glu-COOH) of TS13. This peak is likely to be a degradation product of TS13, and was previously observed in A431 lysates and single cells.[20] Average migration times for the TS13 and fragment peaks were 1220 ± 160 s and 1520 ± 260 s with efficiencies of 5.7 ± 1.1 x 10^4 and 6.6 ± 4.5 x 10^4 theoretical plates and a resolution of 13 ± 4.9. The area of the fragment peak relative to the combined area of all peaks was linearly correlated with incubation time (R^2 = 0.76) (Figure 3.1A) and the degradation rate was linearly correlated with the amount of TS13 injected (R^2 = 0.92) (Figure 3.1B), suggesting first-order reaction

kinetics. Assuming an average protein concentration of 1 g/mL, the median rate of degradation was 43 fmol min^{-1} mg^{-1} (Q_1 and Q_3 of 15 and 82 fmol min^{-1} mg^{-1}, equating to a median half-life of 20 min (Q_1 and Q_3 of 15 and 89 min). This is comparable to the 39 fmol min^{-1} mg^{-1} median rate previously measured in single A431 cells. Reporter degradation in BEAS-2B cells will result in 2-3% breakdown within the 60 s timespan of dephosphorylation experiments so reporter optimization to enhance proteolytic stability was unnecessary.

Measurement of PTP activity in single BEAS-2B cells. To determine the utility of pTS13 for measuring PTP activity in single human airway cells, BEAS-2B cells were microinjected and their contents analyzed by CE-LIF (Figure 3.2). The median amount of reporter introduced into a cell was 1.1 amol (Q_1 = 0.66 amol, Q_3 = 3.0 amol). Robust dephosphorylation was observed, with 90% (n = 10) of the cells completely dephosphorylating the peptide within 60s. While exact rates could not be calculated for cells with no phosphorylation remaining, the median dephosphorylation rate was greater than 2.2 pmol min^{-1} mg^{-1} (Q_1 and Q_3 of 1.1 and 6.0 pmol min^{-1} mg^{-1}). The single BEAS-2B cell that did not fully dephosphorylate the reporter contained 0.7 amol (1.4 μM) of reporter, within the interquartile range for amount loaded, suggesting that incomplete reporter dephosphorylation was not due to excessive loading, but more likely reflects intercellular heterogeneity. Reporter breakdown was negligible over the 60 s time course of these experiments.

Inhibition of PTP activity in single BEAS-2B cells. Treatment of cells with environmental toxins resulted in substantial inhibition of PTP activity in single BEAS-2B cells. Treatment with pervandate (1 mM), Zn^{2+} (100 μM), and 1,2-naphthoquinone (150 μM) resulted in statistically significant PTP inhibition relative to untreated cells ($p < 0.0001$), with medians of 76% (Q_1 = 62%, Q_3 = 86%), 69% (Q_1 = 58%, Q_3 = 73%), and 100% (Q_1 = 95%,

Q_3 = 100%) of the reporter remaining phosphorylated after 60 s. As compared to A431 cells, pervanadate treatment of BEAS-2B cells resulted in greater PTP inhibition ($p = 0.050$) and intercellular heterogeneity, represented by the standard deviation of each sample, was less pronounced ($p = 0.035$). Comparisons between BEAS-2B and A431 cells treated with $Zn2^+$ suggest greater inhibition among BEAS-2B cells, but lacked the statistical power to reach significance ($p = 0.096$). Results of 1,2-naphthoquinone experiments are not directly comparable due to higher toxin concentrations used for BEAS-2B experiments than with A431 cells. These data suggest that the PTPs are more susceptible to toxic inhibition in BEAS-2B cells than in A431, and that the clonal heterogeneity is less pronounced. These conclusions are consistent with the relatively normal biochemical phenotype exhibited by BEAS-2B (discussed above) as well as established links between tumorigenic cell lines and increased heterogeneity.[25]

Lifetime of the PTP reporter in single hAECs. While the PTP reporter is robust to degradation in single BEAS-2B cells, breakdown in primary airway cells may differ. Therefore, the lifetime of the PTP reporter was evaluated in single primary airway epithelial cells by microinjection of TS13 and analysis by CE-LIF. In addition to TS13, a second peak was observed with the same migration time as the 8-residue fragment peak seen in BEAS-2B cells. The area of this fragment peak relative to the combined area of all peaks was linearly correlated with incubation time ($R^2 = 0.83$) (Figure 3.3A). The median amount of reporter injected into cells was 11 amol (22 μM) with Q_1 and Q_3 of 1.0 and 15 amol (2.0 and 30 μM), and a strong linear correlation was observed between the degradation rate and amount of TS13 loaded into a cell ($R^2 = 0.96$) (Figure 3.3B), suggesting first-order degradation kinetics. The median degradation rate was 550 fmol min^{-1} mg^{-1} (Q_1 and Q_3 of 100 and 1700 fmol min^{-}

^{1} mg^{-1}), equating to a median half-life of 28 min (Q_1 and Q_3 of 17 and 44 min) in cells. While the measured degradation rate in primary cells was an order of magnitude greater than seen in BEAS-2B cells, the average amount of peptide measured per cell was proportionately larger as well. The mechanism underlying this disparity is unknown, but is likely due to differences in microinjection efficiency (*i.e.* differential delivery of reporter). No difference was found between reporter half-life in primary hAECs and BEAS-2B ($p = 0.28$), supporting that the apparent rate disparity is a consequence of substrate concentration rather than innate differences in degradative capacity. The similarity in reporter half-life and degradation pattern is consistent with the biochemical similarities between BEAS-2B and primary airway cells discussed earlier.

Measurement of PTP activity in single primary hAECs. Introduction of pTS13 into living cells without the need for genetic manipulation allows direct analysis of primary cells. To demonstrate the value of this technique for measuring PTP activity in primary cells, pTS13 was microinjected into single cultured primary hAECs and dephosphorylation was measured by CE-LIF (Figure 3.4). Exact dephosphorylation rates for 7 of 12 hAECs could not be calculated due to complete dephosphorylation of pTS13 within the 60 s incubation time, but the median dephosphorylation rate was greater than 2.2 pmol min^{-1} mg^{-1} (Q_1 and Q_3 of 0.20 and 18 pmol min^{-1} mg^{-1}). Plots of dephosphorylation rate vs total amount of reporter demonstrate that PTP activity was not saturated across the mass range of reporter delivered (0.1-100 amol), and that dephosphorylation rate is linearly correlated to amount of reporter ($R^2 = 0.99$).

Inhibition of PTP activity in single primary hAECs. Treatment of cells with environmental toxins significantly inhibited PTP activity relative to untreated controls ($p <$

0.0001 for each treatment vs. control). Cells treated with pervanadate, $Zn2^{+}$, and 1,2-naphthoquinone possessed a median of 91% (Q_1 = 86%, Q_3 = 98%), 88% (Q_1 = 87%, Q_3 = 91%), and 87% (Q_1 = 75%, Q_3 = 92%) phosphorylation remaining after 60 s. As compared to BEAS-2B cells, primary airway cells exhibited less inhibition by naphthoquinone (p = 0.0027), but were more susceptible to inhibition by Zn^{2+} (p = 0.0039) and pervanadate (p = 0.0001). While the mechanism underlying these results is not well understood, they may imply a difference between BEAS-2B cells and primary airway cells with respect to antioxidative function, cation transport, or quinone metabolism. Additionally, intercellular heterogeneity of response to treatment, measured as the standard deviation within a treatment group, was less pronounced in primary hAECs treated with pervanadate (p = 0.019 vs. BEAS-2B, p = 0.003 vs. A431) and Zn^{2+} (p = 0.0026 vs. BEAS-2B, p = 0.0161 vs. A431). Decreased heterogeneity in low passage number primary cells is consistent with the previously described development of heterogeneity in clonal populations.[25-26]

Analysis of bronchial brushing specimen. Bronchial brushings obtained from human subjects provide access to primary airway cells that have undergone exposure (e.g. to inhaled pollutants) in the most physiological environment possible. However, analysis of these cells is challenging due to small sample size, low viability, and contamination with undesirable cells and mucus. To demonstrate the applicability of pTS13 to the study of PTP activity in these *ex vivo* samples, single viable epithelial cells from bronchial brushings were identified by vital staining (Figure 3.4A-C), microinjected with pTS13, and analyzed by CE-LIF (Figure 3.4D-F). The amount of pTS13 injected ranged from 1.2-41 amol (2.0-82 μM) and dephosphorylation rate was positively correlated with total amount of reporter (R^2 = 0.99). Dephosphorylation rates ranged from 0.35-36 pmol min^{-1} mg^{-1}, similar to the rates

observed in BEAS-2B and hAECs. Analysis of 3 cells directly obtained from bronchial brushing of a human subject demonstrates the applicability of this technique to the measurement of PTP activity in *ex vivo* airway tissue samples.

Conclusion

A recently developed chemical cytometry reporter of PTP activity was demonstrated to be a valuable tool for the study of human airway cells. Immortalized bronchial epithelia, cultured primary airway epithelia, and unpassaged cells from an *ex vivo* human specimen were microinjected with a fluorescent phosphopeptide and dephosphorylation was quantified using CE-LIF. Inhibition of PTP activity was observed in immortalized and primary cells after treatment with several environmental toxins. Comparison of BEAS-2B and primary hAECs identified statistically significant differences in the response to these toxins, with hAECs showing greater response to both pervanadate and Zn^{2+}, while BEAS-2B cells were more strongly inhibited by 1,2-naphthoquinone. In addition to information about the magnitude of PTP activity and inhibition, analysis of cells individually provided insight into the heterogeneity within populations of BEAS-2B cells and hAECs. Relative to BEAS-2B cells, the variability of response was smaller for hAECs treated with 1 mM pervanadate ($p = 0.019$) or 100 μM Zn^{2+} ($p = 0.0026$). Achieving statistical significance for comparisons of variability between populations is typically challenging, especially with small samples sizes, further demonstrating the power of this technique. Finally, the pre-selection of viable epithelial cells for analysis was critical to the successful analysis of the heterogeneous, size-limited *ex vivo* specimen. While the sample size achieved in these experiments was

insufficient to draw biological conclusions, these analyses have demonstrated a unique new approach to studying PTP signaling in challenging primary samples.

Signaling of PTPs is vitally important to cell physiology and the ability to measure PTP activity in *ex vivo* specimens will be a valuable tool for the study of conditions including cardiovascular and metabolic disease, immune dysfunction, and cancer. It is increasingly clear that that no single approach is sufficient to decode the complexity of cell signaling, and direct enzyme activity measurement may be used to develop functional biomarkers of disease and pharmacodynamic readouts of exposure to toxins and therapeutics alike.

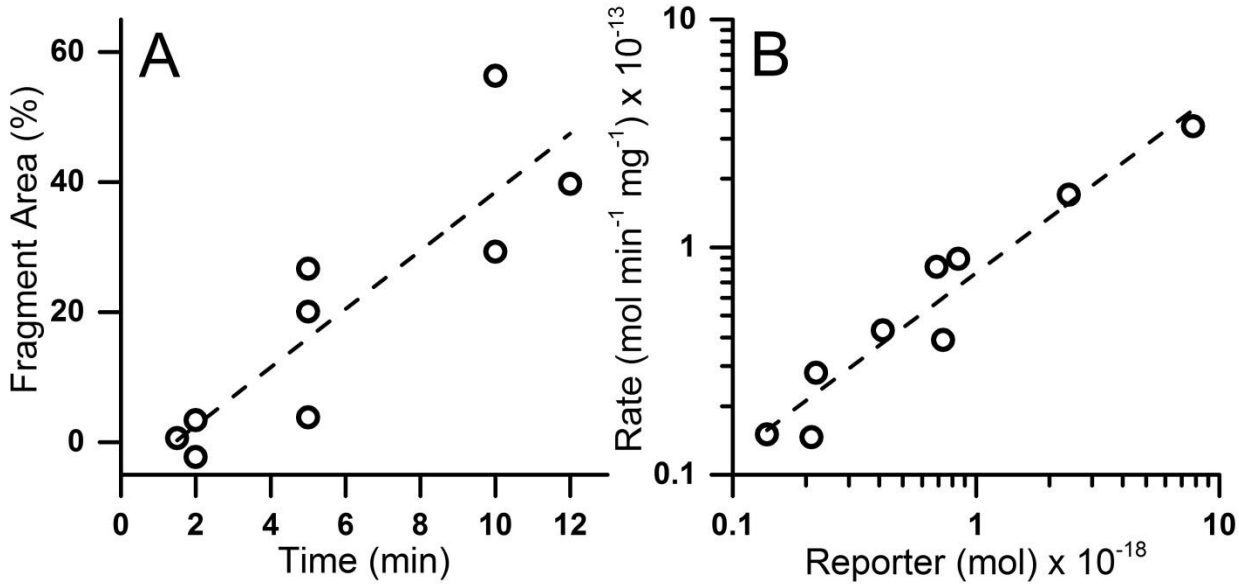

Figure 3.1. Fragmentation of TS13 in single BEAS-2B cells. Each symbol represents the measurement from a single cell. A) The percentage of the peak area of the fluorescent 8-residue fragment with respect to the total peptide loaded into the cells was plotted over time. B) Rate of conversion of TS13 to the 8-residue fragment was plotted against the total amount of TS13 loaded into a cell. Dashed lines indicate linear regression with $R^2 = 0.76$ (A) and 0.92 (B).

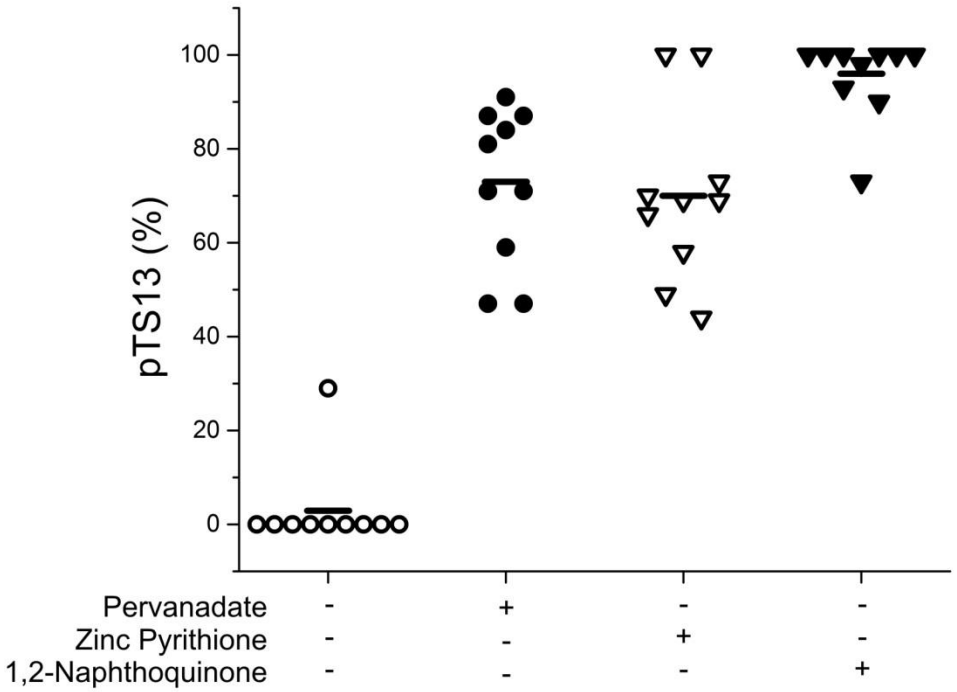

Figure 3.2. PTP activity in single BEAS-2B cells. PTP activity was assessed in single BEAS-2B cells in the absence of toxins (◦) or after pretreatment with 1 mM pervanadate (•), 100 μM Zn^{2+} (▽), or 150 μM 1,2-naphthoquinone (▼) for 10 min. Dashes indicate mean phosphorylation remaining after 60 s. Each symbol marks the measurement from a single cell and the y-axis reflects the percentage of pTS13 relative to the total TS13 and pTS13.

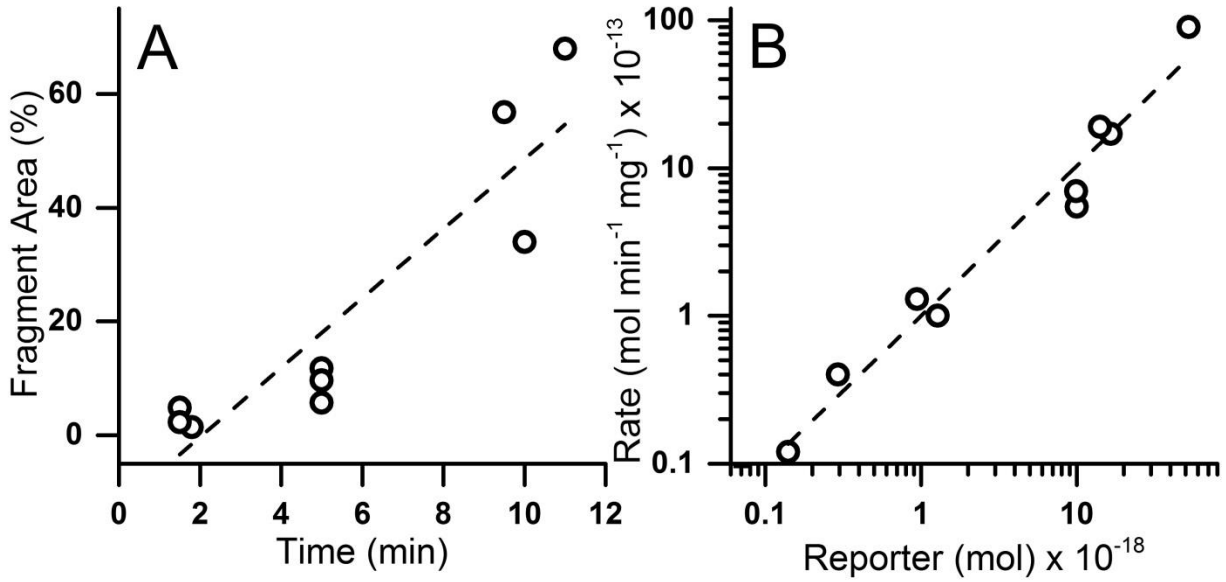

Figure 3.3. Fragmentation of TS13 in single hAECs. Each symbol represents the measurement from a single cell. A) The percentage of the peak area of the fluorescent 8-residue fragment with respect to the total peptide loaded into the cells was plotted over time. B) Rate of conversion of TS13 to the 8-residue fragment was plotted against the total amount of TS13 loaded into a cell. Dashed lines indicate linear regression with $R^2 = 0.83$ (A) and 0.96 (B).

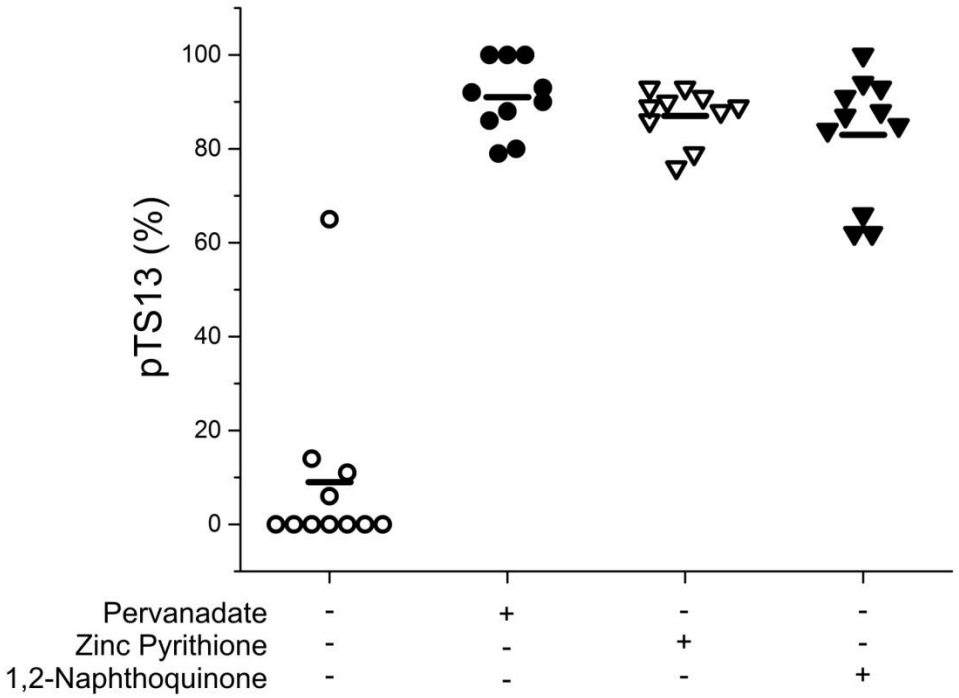

Figure 3.4. PTP activity in single hAECs. PTP activity was assessed in single hAECs in the absence of toxins (◦) or after pretreatment with 1 mM pervanadate (•), 100 μM Zn^{2+} (▽), or 150 μM 1,2-naphthoquinone (▼) for 10 min. Dashes indicate mean phosphorylation remaining after 60 s. Each symbol marks the measurement from a single cell and the y-axis reflects the percentage of pTS13 relative to the total TS13 and pTS13.

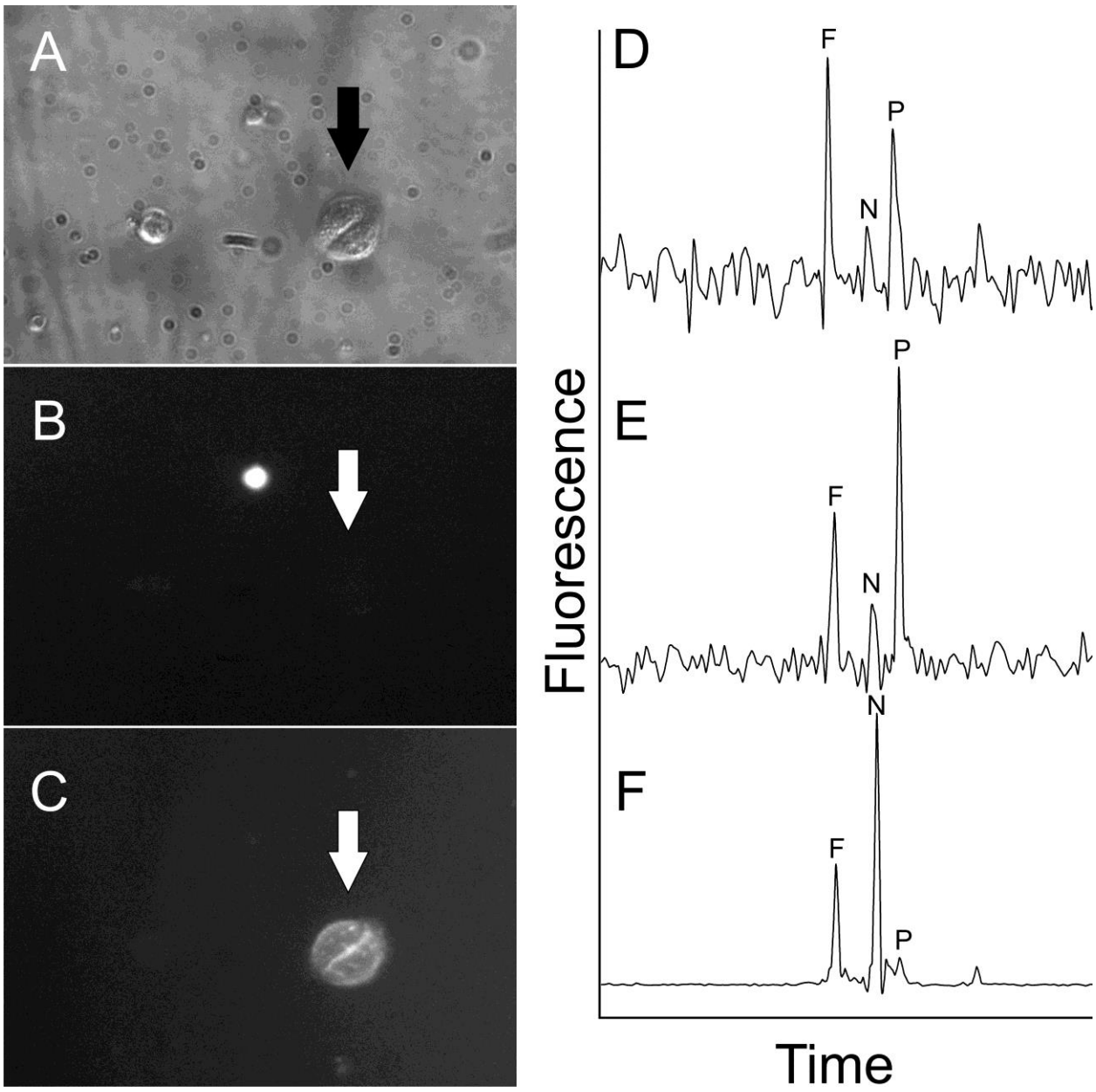

Figure 3.5. Analysis of PTP activity in bronchial brushing specimens. Viable epithelial cells from a bronchial brushing specimen were identified, microinjected with pTS13, and analyzed by CE-LIF. After immunofluorescent staining, cells of interest were visualized using bright field (A) as well as fluorescence microscopy using Cy3 (B) and Cy5 (C) filter sets to assess viability and EpCAM expression. Cells were then microinjected with a 6-

FAM/pTS13 mixture and analyzed by CE-LIF after 60 s [electrophoretic traces shown in (D-F)]. Labeled peaks represent 6-FAM ("F"), TS13 ("N"), and pTS13 ("P"). Axes have been normalized to correct for migration time variability and signal intensity.

References

1. Heron, M., *Natl Vital Stat Rep,* **2012,** *60,* 1-94.

2. Bartoli, C. R.; Wellenius, G. A.; Diaz, E. A.; Lawrence, J.; Coull, B. A.; Akiyama, I.; Lee, L. M.; Okabe, K.; Verrier, R. L.; Godleski, J. J., *Environ Health Perspect,* **2008,** *117*.

3. Liao, D.; Duan, Y.; Whitsel, E. A.; Zheng, Z. J.; Heiss, G.; Chinchilli, V. M.; Lin, H. M., *Am J Epidemiol,* **2004,** *159,* 768-777.

4. Miller, K. A.; Siscovick, D. S.; Sheppard, L.; Shepherd, K.; Sullivan, J. H.; Anderson, G. L.; Kaufman, J. D., *N Engl J Med,* **2007,** *356,* 447-458.

5. Samet, J. M.; Rappold, A.; Graff, D.; Cascio, W. E.; Berntsen, J. H.; Huang, Y. C.; Herbst, M.; Bassett, M.; Montilla, T.; Hazucha, M. J.; Bromberg, P. A.; Devlin, R. B., *Am J Respir Crit Care Med,* **2009,** *179,* 1034-1042.

6. Pourazar, J.; Mudway, I. S.; Samet, J. M.; Helleday, R.; Blomberg, A.; Wilson, S. J.; Frew, A. J.; Kelly, F. J.; Sandstrom, T., *Am J Physiol Lung Cell Mol Physiol,* **2005,** *289,* L724-730.

7. Wang, T.; Chiang, E. T.; Moreno-Vinasco, L.; Lang, G. D.; Pendyala, S.; Samet, J. M.; Geyh, A. S.; Breysse, P. N.; Chillrud, S. N.; Natarajan, V.; Garcia, J. G., *Am J Respir Cell Mol Biol,* **2009**.

8. Lee, S. R.; Kwon, K. S.; Kim, S. R.; Rhee, S. G., *J Biol Chem,* **1998,** *273,* 15366-15372.

9. Tal, T. L.; Bromberg, P. A.; Kim, Y.; Samet, J. M., *Toxicol Appl Pharmacol,* **2008,** *233,* 382-388.

10. Stewart, C. E.; Torr, E. E.; Mohd Jamili, N. H.; Bosquillon, C.; Sayers, I., *J Allergy (Cairo),* **2012,** *2012,* 943982.

11. Romagnoli, M.; Vachier, I.; Vignola, A. M.; Godard, P.; Bousquet, J.; Chanez, P., *Respir Med,* **1999,** *93,* 461-466.

12. Yendamuri, S.; Vaporciyan, A. A.; Zaidi, T.; Feng, L.; Fernandez, R.; Bekele, N. B.; Hofstetter, W. L.; Jiang, F.; Mehran, R. J.; Rice, D. C.; Spitz, M. R.; Swisher, S. G.; Walsh, G. L.; Roth, J. A.; Katz, R. L., *J Thorac Oncol,* **2008,** *3,* 979-984.

13. Bewig, B.; Haacke, T. C.; Tiroke, A.; Bastian, A.; Bottcher, H.; Hirt, S. W.; Rautenberg, P.; Haverich, A., *Respiration,* **2000,** *67,* 166-172.

14. Yang, I. V.; Tomfohr, J.; Singh, J.; Foss, C. M.; Marshall, H. E.; Que, L. G.; McElvania-Tekippe, E.; Florence, S.; Sundy, J. S.; Schwartz, D. A., *Am J Respir Crit Care Med,* **2012,** *185,* 620-627.

15. Hamilton, L. M.; Puddicombe, S. M.; Dearman, R. J.; Kimber, I.; Sandstrom, T.; Wallin, A.; Howarth, P. H.; Holgate, S. T.; Wilson, S. J.; Davies, D. E., *Eur Respir J,* **2005,** *25,* 978-985.

16. Lin, Y.; Trouillon, R.; Safina, G.; Ewing, A. G., *Anal Chem,* **2011,** *83,* 4369-4392.

17. Lu, C., *Chemical cytometry : ultrasensitive analysis of single cells*. Wiley-VCH: Weinheim, 2010; p xix, 247 p.

18. Whitmore, C. D.; Olsson, U.; Larsson, E. A.; Hindsgaul, O.; Palcic, M. M.; Dovichi, N. J., *Electrophoresis,* **2007,** *28,* 3100-3104.

19. Essaka, D. C.; Prendergast, J.; Keithley, R. B.; Hindsgaul, O.; Palcic, M. M.; Schnaar, R. L.; Dovichi, N. J., *Neurochem Res,* **2012,** *37,* 1308-1314.

20. Phillips, R. M.; Blair, E.; Lawrence, D. S.; Sims, C. E.; Allbritton, N. L., *Anal Chem,* **2013**.

21. Gill, G. N.; Weber, W.; Thompson, D. M.; Lin, C.; Evans, R. M.; Rosenfeld, M. G.; Gamou, S.; Shimizu, N., *Somat Cell Mol Genet,* **1985,** *11,* 309-318.

22. Kinnula, V. L.; Yankaskas, J. R.; Chang, L.; Virtanen, I.; Linnala, A.; Kang, B. H.; Crapo, J. D., *Am J Respir Cell Mol Biol,* **1994,** *11,* 568-576.

23. McGovern, T.; Risse, P. A.; Tsuchiya, K.; Hassan, M.; Frigola, G.; Martin, J. G., *Am J Physiol Lung Cell Mol Physiol,* **2010,** *299,* L808-815.

24. Heijink, I. H.; Brandenburg, S. M.; Noordhoek, J. A.; Postma, D. S.; Slebos, D. J.; van Oosterhout, A. J., *Eur Respir J,* **2010,** *35,* 894-903.

25. Masramon, L.; Vendrell, E.; Tarafa, G.; Capella, G.; Miro, R.; Ribas, M.; Peinado, M. A., *J Cell Sci,* **2006,** *119,* 1477-1482.

26. Brock, A.; Chang, H.; Huang, S., *Nat Rev Genet,* **2009,** *10,* 336-342.

IV. Conclusions and Future Directions

The protein tyrosine phosphatase (PTP) activity assay described in chapters 2 and 3 is a powerful new tool for the study of cell signaling. By measuring enzyme activity in single cells directly through substrate dephosphorylation, this approach provides a number of benefits. One important advantage of single-cell analysis is the preservation of data describing intercellular heterogeneity, information that is lost when analyzing bulk lysates. To date, this technique has provided the statistical power necessary to identify differences in intercellular heterogeneity in relatively small samples sizes ($n \leq 10$). Analysis of single cells also provides the opportunity to identify rare subpopulations of cells, the likelihood of which is related to the prevalence of that subpopulation within the sample. For example, if a subpopulation represents 1% of the whole, the probability of identifying one cell from that subpopulation is 0.1 for $n = 10$, but 0.87 for $n = 200$. As this technology matures, a focus on increased throughput will provide greater statistical power for describing population characteristics (e.g. central tendency, variance, shape of distribution) as well as for comparisons between populations. This will also be especially valuable for studying subtle differences in signaling, such as characterizing response to low concentrations of toxins or drugs, or identifying differences between similar populations.

An automated single-cell CE system has recently been developed, capable of analyzing 2.1 cells/min for 219 consecutive cells.[1] This high-throughput system was used to measure sphingosine kinase activity by CE-LIF in single cells residing in microfabricated

wells. To date, microinjection has not been integrated into this system, but automated microinjection systems with a throughput of 0.9 cells/min have been described.[2] Higher throughput for single-cell CE may also be achievable through the adaptation and inclusion of capillary arrays. Detection limits on the order of 10^{-21} mol for fluorescein and 10^{-20} for fluorescent sphingolipids have been reported for a parallel array of 32 capillaries performing CE simultaneously.[3] High throughput microfluidic chemical cytometry (0.6 cells/min for an average of 50 single cells per experiment) has also been recently reported.[4] In this system, electrophoretic separation of peptide reporter species, including breakdown products, takes place in a microfluidic channel rather than a capillary. The integration of vital staining to identify cells of interest could allow focused analysis of large numbers of primary cells without the need for attachment to a substrate, though replacement of microinjection with an alternative reporter loading technique would also be necessary. The integration of one or more of these approaches with the PTP activity reporter may substantially increase throughput.

Another key advantage of this approach is the quantification of both substrate and product, which provides valuable information about PTP rates. We have demonstrated that significant changes in dephosphorylation rate occur in A431, BEAS-2B, and primary airway cells in response to toxic inhibition. The 500 fL average volume of a mammalian cell[5] places inherent limitations on the amount of reporter than can be introduced into a single cell. Limits of detection on the order of 10-^{21} mol[6] for capillary electrophoresis with laser-induced fluorescence detection (CE-LIF) are well suited to the quantification of analytes on the scale of the single cell. An implication of this reporter mass limitation is that it establishes a finite time window after which the PTP reporter is completely dephosphorylated. As reported in

chapters 2 and 3, when only one reporter species is detectable at the time of analysis, the exact rate of dephosphorylation cannot be calculated because the actual reaction time is unknown. This phenomenon creates a statistical floor effect in which the true distribution of data is unknowable. This effect is inconsequential for comparisons of clearly distinct populations, but reduces statistical power when dephosphorylation is very rapid in multiple populations.

A potential avenue for increasing the temporal resolution of this technique, and thus its analytical power, is the development of a caged PTP substrate that can be dephosphorylated only after photolysis. Caged phosphotyrosine has been synthesized and shown to uncage upon light exposure after inclusion in peptides using solid phase peptide synthesis.[7-9] The ability to control the initiation of reporter dephosphorylation could permit considerably shorter time points. A possible alternative method of addressing the floor effect resulting from rapid reporter dephosphorylation would be to use apply iterative peptide sequence modification, previously demonstrated to increase phosphorylation rates of kinase substrates,[10] to create a sequence that is dephosphorylated more slowly, thereby increasing the time window available for observation of partial dephosphorylation.

The tunability of peptide substrates combined with the high resolution, high peak capacity analytical separations afforded by CE-LIF provide great potential for future development of this approach to address increasingly complex biological questions. CE provides the capacity to separate multiple analytes based on small differences in charge and hydrodynamic radius, and has been used to detect as many as 20 analytes simultaneously using single-color detection.[11] This separation capacity combined with the capacity for

multi-color detection[12] make possible the quantification of multiple enzyme activities in a single cell, leading to a better understanding of signaling networks and pathways.

In conclusion, the PTP reporter described herein allows quantification of PTP activity as well as intercellular heterogeneity in a variety of cell populations, up to and including the small, heterogeneous populations of primary cells obtained from human subjects by bronchial brushing. The combination of well-established methods such as solid phase peptide synthesis and capillary electrophoresis with leading-edge single-cell analysis technology provides a powerful and highly flexible tool for the study of PTP signaling at the single cell level. This tool is directly applicable to the study of airway cells from human subjects, and has significant potential for future development.

References

1. Dickinson, A. J.; Armistead, P. M.; Allbritton, N. L., *Anal Chem,* **2013**.

2. Graf, S. F.; Madigou, T.; Li, R.; Chesne, C.; Stemmer, A.; Knapp, H. F., *J Lab Autom,* **2011,** *16,* 186-196.

3. Dada, O. O.; Ramsay, L. M.; Dickerson, J. A.; Cermak, N.; Jiang, R.; Zhu, C.; Dovichi, N. J., *Anal Bioanal Chem,* **2010,** *397,* 3305-3310.

4. Kovarik, M. L.; Shah, P. K.; Armistead, P. M.; Allbritton, N. L., *Anal Chem,* **2013,** *85,* 4991-4997.

5. Schmid, A.; Kortmann, H.; Dittrich, P. S.; Blank, L. M., *Curr Opin Biotechnol,* **2010,** *21,* 12-20.

6. Whitmore, C. D.; Olsson, U.; Larsson, E. A.; Hindsgaul, O.; Palcic, M. M.; Dovichi, N. J., *Electrophoresis,* **2007,** *28,* 3100-3104.

7. Rothman, D. M.; Vazquez, M. E.; Vogel, E. M.; Imperiali, B., *J Org Chem,* **2003,** *68,* 6795-6798.

8. Humphrey, D.; Rajfur, Z.; Vazquez, M. E.; Scheswohl, D.; Schaller, M. D.; Jacobson, K.; Imperiali, B., *J Biol Chem,* **2005,** *280,* 22091-22101.

9. Goguen, B. N.; Aemissegger, A.; Imperiali, B., *J Am Chem Soc,* **2011,** *133,* 11038-11041.

10. Proctor, A.; Wang, Q.; Lawrence, D. S.; Allbritton, N. L., *Anal Chem,* **2012,** *84,* 7195-7202.

11. Piccard, H.; Hu, J.; Fiten, P.; Proost, P.; Martens, E.; Van den Steen, P. E.; Van Damme, J.; Opdenakker, G., *Electrophoresis,* **2009,** *30,* 2366-2377.

12. Keithley, R. B.; Rosenthal, A. S.; Essaka, D. C.; Tanaka, H.; Yoshimura, Y.; Palcic, M. M.; Hindsgaul, O.; Dovichi, N. J., *Analyst,* **2013,** *138,* 164-170.